

Adapting an Existing Batch Pulp Digester Model for Use in Continuous Digesters

Johannes Daniël de Bruin

Adapting an Existing Batch Pulp Digester Model for Use in Continuous Digesters

by

Johannes Daniël de Bruin

A dissertation submitted in partial fulfillment of the requirements for the degree

Master of Engineering (Control Engineering)

in the

Department of Chemical Engineering
Faculty of Engineering, the Built Environment and Information
Technology

University of Pretoria

Pretoria

December 2020

Abstract

A mathematical model of a continuous Kraft wood digester was developed and tested. The model relies heavily on the work done previously by Christensen, Albright & Williams (1982). The batch Kraft digester model developed by Christensen *et al* (1982) was adapted to model a continuous Kraft wood digester at Ngodwana, South Africa. This adaptation centres around utilizing the method of lines to account for changes in both time and height of the digester simultaneously. The model was able to simulate the Kappa number of the digester accurately to an average absolute error of 7.88 that was reduced to 2.87 after certain process parameters were optimized for. A moving horizon state estimator was introduced into the model in an effort to keep internal state prediction accurate. This addition brought the average absolute error down further to 2.75. Adaptive control was also implemented into the model. The plant data the model was compared against to determine its accuracy was filtered with the use of a rolling median filter to reduce the influence introduced by noisy and infrequent measurements.

Keywords: Kappa number, Kraft digester, Continuous digester model, Sappi, Ngodwana

Acknowledgements

I would like to acknowledge the encouragement, help and motivation of my fiancée and her family, my father and my grandparents, the exceptional and enriching guidance of Carl Sandrock and the eager willingness of Nico Brunke and Justin Phillips to aid in any need of communication. I would also like to thank Freddie Grobler who was instrumental in gaining understanding and data of the digester and plant and Wayne Davis for his indispensable drive to bring this project to fruition. I also want to thank Sappi Ngodwana for funding this project and, without whom, none of this would be possible. Lastly I want to thank my heavenly Father for His guidance and the strength He provides me with.

I lift my eyes unto the hills -
Where does my help come from?
My help comes from the Lord
The Maker of heaven and earth

-Psalms 121:1-2

Contents

Synopsis	i
Nomenclature	viii
1 Introduction	1
1.1 Background	1
1.2 Problem statement	2
1.3 Aim	2
1.4 Method	3
1.5 Scope and issues	3
2 Theoretical background	4
2.1 Sappi	4
2.2 Wood	4
2.2.1 Cellulose	5
2.2.2 Hemicellulose	5
2.2.3 Lignin	5
2.2.4 Wood types	6
2.3 Pulping	7
2.3.1 Mechanical pulping	7
2.3.2 Chemical pulping	7
2.3.3 Sulphite pulping	9
2.3.4 Sulphate (Kraft) process	9
2.3.5 Cooking procedure	10
2.4 Modelling and control	11
2.4.1 Modelling	12
2.4.2 Batch models vs continuous models	16
2.5 UP model	16
2.5.1 Reaction rates	17
2.5.2 Liquor composition	18
2.6 Continuous model history	20
2.6.1 Groundwork of the Purdue model	20
2.6.2 Further innovation	21
2.7 Kraft model	22
2.8 Method of lines as a partial derivative solution technique	25
2.8.1 Partial differential equations	25
2.8.2 Method of lines	26
2.9 State estimation	26

2.9.1	Modified Kalman filters	27
2.9.2	Moving horizon estimation	27
2.9.3	Comparison of state estimators	29
2.10	Adaptive control	29
2.10.1	Parameter drift	29
2.10.2	Parameter optimization	30
3	Model decision	31
3.1	Preface	31
3.2	Model comparison	31
3.3	Kraft model selection	32
3.4	Kraft model	33
4	Continuous model	35
4.1	Continuous digester modelling needs	35
4.2	Process schematic diagram	35
4.2.1	Model inputs	37
4.2.2	Model outputs	38
4.2.3	Kappa Measurements	38
4.3	Modelling assumptions	39
4.4	Spatial variations	42
4.5	Model composition	42
4.5.1	Variables used	43
4.5.2	Inputs	46
4.5.3	Reaction kinetics	48
4.5.4	Reactor dynamics	50
4.5.5	Simulation	51
4.5.6	Results	52
4.6	Model synthesis	56
4.7	Degrees of Freedom analysis	57
4.8	Model simplification	58
4.9	Input distinction	58
4.10	Simulation Addition	59
5	Results	61
5.1	Preliminary model testing	61
5.2	Plant data comparison	64
6	Model enhancements	72
6.1	State estimation	72

6.1.1	Need for state estimation	72
6.1.2	Method	73
6.1.3	Results	74
6.2	Adaptive control	74
7	Data handling	76
7.1	Data processing	76
7.2	Kappa number measurements	76
7.2.1	Kappa measurement inconsistency	77
7.2.2	Solution	79
8	Conclusion	80

List of Figures

1	Moving horizon estimation using a system model and optimization to reconcile past measurements over a horizon of length N	28
2	Schematic of the digester layout.	36
3	Schematic of the cooking section.	37
4	Kappa analyser 1, 2 and 3 location in relation to the digester.	39
5	Illustration of CSTR approximation of digester.	43
6	Wood components in CSTR over time.	54
7	Caustic solution and temperature over time.	55
8	Illustration of the CSTR approximation with respect to volume and time.	57
9	Wood component mass over volume of digester with steady state inputs.	62
10	Caustic solution and temperature over digester volume with steady state inputs.	63
11	Kappa number predicted compared to real plant data.	64
12	Parity plot of Kappa number predicted compared to real plant data.	65
13	Kappa number predicted by optimized parameters compared to real plant data.	68
14	Parity plot showing Kappa number predicted by optimized parameters compared to real plant data.	69
15	Kappa number predicted by Set 1 parameters compared to real plant data.	70
16	Kappa number predicted by Set 2 parameters compared to real plant data.	70
17	Kappa number predicted by Set 3 parameters compared to real plant data.	71
18	Kappa number predicted by optimized parameters with MHE initial values compared to real plant data.	74
19	Exaggerated examples of the possibilities introduced by adaptive control.	75
20	Kappa analyser 1, 2 and 3 location in relation to the digester.	77
21	Kappa measurements over time for a randomly chosen data set.	78
22	Parity plot showing similarity between Kappa measurements over time for a randomly chosen data set.	78

List of Tables

1	Hard- and softwood ODW compositions (Rydholm, 1965).	7
2	Variables used by the UP model.	19
3	Christensen, Albright & Williams (1982) model variables.	24
4	Christensen, Albright & Williams (1982) model equations.	33
5	Model inputs.	37
6	Model outputs.	38

7	Model parameters.	44
8	Kinetic Reaction Parameters by Wisnewski, Doyle & Kayihan (1997). . .	44
9	Intermediate variables.	45
10	Input parameters.	46
11	Model outputs.	46
12	Used Python libraries.	52
13	Initial values to CSTR simulation.	53
14	Distinction between state and flow variables in CSTR.	56
15	Initial values to steady input digester simulation.	61
16	Parameters used in fitting.	68
17	States of every CSTR segment in digester.	73
18	Measures of Kappa measurement similarity.	78

Nomenclature

CSTR Continuous stirred tank reactor

DOF Degrees of Freedom

EKF Extended Kalman filter

MHE Moving horizon estimation

MOL Method of lines

MPC Model predictive control

ODE Ordinary differential equation

ODW Oven dried wood

PDE Partial differential equations

PFR Plug flow reactor

UKF Unscented Kalman filter

1 Introduction

Since the dawn of the paper making process, one of the first steps involve creating a pulp from a fibrous substance such as wood. In modern times, this pulping step is often done with the use of a wood pulp digester. This is no different at Sappi, South Africa, where around 700 000 tons of paper is produced annually.

1.1 Background

Since 1999, the University of Pretoria's Chemical Engineering Department has been involved with the Saiccor mill in KwaZulu-Natal, South Africa owned by Sappi. Saiccor utilizes batch digesters to create wood pulp. In an effort to reduce variability in the pulp quality, it was deemed necessary to control various variables in the batch process. These are variables such as: the time the batch takes, the amount of solvent added and the temperature of the batch, to name a few. In order to control such a large, highly interacting system it was decided that a mathematical model of the reaction kinetics of the process would be helpful. With this, control systems such as model predictive control (MPC) could be implemented to control the quality of the pulp (Kilian, 1999). This model was developed by Kilian (1999) and is known as the UP model (named after the University of Pretoria). It is used to model the DP throughout the batch (also called a cook). This model had been greatly expanded on since 1999 and, in its current state, it is reasonably accurate for the system (Stephens, 2017).

Sappi owns 5 mills in South Africa. Two of these are the aforementioned Saiccor mill and the Ngodwana mill in Mpumalanga. This second mill has been dissolving wood for paper since its construction in 1966. These are the two mills of concern for this dissertation as the viability of adapting the UP model for use on the Ngodwana plant will be investigated. One of the differences between the Ngodwana mill and the Saiccor mill is that Ngodwana utilizes continuous digesters while Saiccor relies on batch digesters (Sappi, 2020). Ngodwana also uses the Kraft process, whereas Saiccor uses the Sulphite process.

Wood consists of 3 main components, cellulose, hemicellulose and lignin (Ek, Gellerstedt & Henriksson, 2009a). To make paper pulp, wood needs to be reduced to individual cellulose fibres. Lignin serves to bind cellulose fibres together and needs to be removed during the pulping process (Ek *et al.*, 2009a). Chemical pulping dissolves most of the lignin and the hemicellulose from the wood, resulting in better separation of the cellulose fibres and better quality pulp. The pulping process takes place in a pulping reactor,

called a digester. The quality of the pulp is determined by either measuring the amount of residual lignin in the pulp, or by measuring the length of the cellulose chains in the pulp. This length is often referred to as the degree of polymerization (DP) (Ek, Gellerstedt & Henriksson, 2009b). From the residual lignin the Kappa number can be determined. The Kappa number gives an indication of the residual lignin content of the pulp and is often used to report pulp quality.

1.2 Problem statement

After wood has been pulped, there will still be some residual lignin remaining. This is because the cellulose fibres are degraded too much if all the lignin is removed (Ek *et al*, 2009b). The lignin content of paper is what gives it its strength, therefore paper with higher lignin content is going to be stronger but less refined. This quality of the produced pulp can be measured in various ways, the most common of which being the measurement of the residual lignin content. The Kappa number of pulp is related to the residual lignin content of the pulp and therefore the Kappa number is often used to represent the quality of the pulp.

It was found that the Kappa number output variability on Sappi's Ngodwana mill is too large. Because of this, they tend to yield products that have Kappa numbers outside the acceptable range of specification. The result is lower predictability of pulp quality as well as a lower yield. In order to reduce the residual lignin variance, it will be necessary to implement better control schemes on the digester. It was decided that a model will allow for better simulation of the process and aid in making decision regarding the operation of the digester.

1.3 Aim

A kinetic model of the batch process already exist as the UP model. It was suggested that the UP model be adapted for use in predicting the dynamics of the continuous digesters at Ngodwana. It is believed that the wood being used in both digesters are similar enough that the reaction kinetics section of the model would remain the same for both. Therefore, only the spatial section of the model would need to be adapted to suit the continuous nature of the Ngodwana digester. The aim of the project is to either adapt the batch digester model of Saiccor for use on the continuous process at Ngodwana, or if the differences in the systems are too extreme, implement a model from literature. This model will then be used to predict the Kappa variance and these predictions will then be used to reduce the Kappa variability.

1.4 Method

The problem needs to be addressed with the development of a model. A literature study will be done to become acquainted with the relevant knowledge on the subject of wood pulping as well as digester modelling (Both Kraft and Sulphite and Batch as well as continuous). The further aim of the literature study will be to compare the UP model to pre-existing continuous Kraft digester models. This comparison will then be used to determine whether the UP model will be adapted or if a model will need to be developed from an alternative source. The relevant starting model will be selected and adapted. These adaptations will likely involve adding hydraulic mass balance equations to batch models, as well as expanding energy balances to account for mass flow. The model will then be coded into simulation software (using Python). This resulting simulation will then be compared to measured plant data to determine the model accuracy. The model parameters and variables will then be optimized to ensure the best possible model accuracy. Further model improvements will be investigated to improve accuracy. The main technique that will be investigated will be to use a state estimator to ensure reasonable initial values to the simulation as well to ensure that the model state drift is limited. Adaptive control will also be investigated to ensure that variables assumed to be parameters change at some after some time to better reflect the true system.

1.5 Scope and issues

The scope of this project only extends to the adaption and development of a model. The following items are explicitly not included in the scope.

- Any design or implementation of any control system.
- Implementation and change management
- Hardware and bespoke software that might become necessary.

As with any project, there are potential limitations of the project are. These are:

- Quality and quantity of available plant data
- Available computational power of the control computer to simulate a complex model.

2 Theoretical background

The paper pulping process was first described by Cai Lun, a 2nd-century CE Han court eunuch (Eliot & Rose, 2009). Since then, the technology of paper pulp production had been refined to produce the quality of paper available today. In modern times, the chemistry and physical mechanisms of paper pulp production is well-established, allowing for greater control over paper quality as well as allowing for the mass scale production of quality paper. Sappi, South Africa provides the world with around 700 000 tons of paper annually.

2.1 Sappi

South African Pulp and Paper Industries Limited (Sappi) is a global company that produces dissolving wood pulp (DWP), paper pulp, paper and various other paper-based products. They own 5 mills across South Africa. They are the Saiccor mill, Tugela mill, Stranger mill, Ngodwana mill and Lomati sawmill. Sappi has access to over 5000 square kilometres of forests, and they produce over 600 kilotons of paper, over 600 kilotons of paper pulp and more than a million tons of DWP annually. With this, they are the world's largest manufacturer of DWP. Sappi acquired Saiccor in 1989 where DWP was produced to export. Sappi finished building Ngodwana in 1966. Ngodwana now produces 330 000 tons per annum of paper pulp for their own consumption, 250 000 tons of DP per annum and 380 000 tons of paper mainly used for newsprint and kraft liner board that is used for packaging per annum. About 70 % of the mill's product is exported with the rest being used locally.

The mill generates its own power in the form of steam and electricity from renewable and other sources. On average, the mill produces more energy than it uses and therefore it exports power to the national grid.

2.2 Wood

All woods contain the same 3 basic components: cellulose, hemicellulose and lignin (Ek *et al*, 2009a). These all lend their unique properties to wood, making wood the durable and strong material it is. These properties are, however, not always desired in paper. This leads to a demand for understanding the physical and chemical properties of both wood and paper.

2.2.1 Cellulose

Cellulose is the main structural component of the cell walls of all true plants. Because of the abundance of plant material, cellulose is the single most common bio-compound on earth (Ek *et al*, 2009a). Cellulose is a natural polymer with glucose as its monomers. The degree of polymerization of glucose tend to be very high. Values of 15 000 residues in one chain are reported and this makes cellulose one of the longest of known polysaccharides. These long fibre strands are the main component in paper and it owes its strength to the length of the polymer chain. Celluloses consist of very straight and unbranched molecule and are often referred to as fibres. Cellulose typically make up 40 % to 50 % of the wood (Rydholm, 1965)

2.2.2 Hemicellulose

Hemicellulose usually make up 20 % to 35 % of the dry mass of wood, depending on the species of tree used. While cellulose has a crystalline structure with long chains (7000 units to 15 000 units), hemicellulose is amorphous and has shorter chains (500 units to 3000 units) (Gibson, 2012). Hemicellulose is found in the matrix between cellulose fibrils in the cell walls. It has been proved in several processes that hemicellulose is difficult to separate from cellulose and lignin without modifying the hemicellulose (Ek *et al*, 2009a). There is a wide variety of different types of hemicellulose. The main monomers of hemicellulose are, hexoses (glucose, mannose and galactose) and or pentoses (xylose and arabinose) along with small quantities of other organic components. The chemical and thermal stability of hemicellulose is generally lower than those of cellulose. Hemicellulose (especially arabinogalactans) tend to branch much easier than cellulose which tends to be unbranched.

2.2.3 Lignin

Lignin makes up 15 % to 35 % of the dry mass of wood. Lignin is a hydrophobic polymer that fills the space between cellulose microfibrils and hemicellulose. This fixes them to each other. Lignin hereby stiffens the wood and gives it rigidity. In contrast, cotton, for example, is a lot softer and more flexible than wood, even though cotton is also mostly cellulose. This is because cotton lacks great amounts of lignin. With lignin in the wood matrix, wood is often referred to as a micro-composite type material, with cellulose being the enforcing fibres and lignin playing the role of a phenolic plastic. Even though lignin is a very abundant polymer, it is quite complex biochemically speaking. Lignin is neither a polysaccharide, a lipid, a protein, nor a nucleotide. Rather, it is polymer with a mixture of aromatic and aliphatic moieties. It is not a linear polymer like cellulose, nor a branched polymer like hemicellulose but rather it is a three-dimensional web with the monomers connected with a number of different ether and carbon-carbon bonds that are randomly

distributed (Ek *et al*, 2009a).

2.2.4 Wood types

Wood is generally divided into 2 categories based on its botanical classification. These categories are hardwoods (often called angiosperms) and the coniferous softwood trees (often referred to as gymnosperms). The classification is based on the seed type of the tree, rather than on the hardness of the wood. That being said, the wood from hardwoods are typically harder than the wood from softwoods. There are many differences between hard- and softwoods. The main differences that influence pulping are discussed below:

Softwood

Softwoods tend to grow faster than hardwoods and because of this they are typically more readily available (Patt & Kardsachia, 1991). Softwoods are typically a more uniform raw material, they have better stem formation, and they are also easier to debark. Their wood consist of longer fibres than those of hardwoods, and they produce higher yields in acidic cooking. The pulp from softwoods posses better wet web strength and better drainage properties than their hardwood counterparts. The paper from softwoods typically posses high strength properties, especially when looking at tear strength, and better runability.

Hardwood

Hardwoods on the other hand also have numerous positive qualities, such as higher stock stability and extremely high growth rate in some cases. Hardwoods posses a higher specific weight, leading to lower transport costs, higher digester capacity as well as higher pulp output. They also have a lower lignin content, leading to easier pulping that is cheaper, looking at both energy consumption and chemical chemicals consumed. They produce high yields in alkaline pulping. The pulp from hardwoods requires less beating energy, shows rapid strength development during beating and has better bleachability. This leads to fewer bleaching stages, lower chemical demand and less pollution.

Wood composition

The average composition of hard- and softwoods are given in Table 1 below:

Table 1: Hard- and softwood ODW compositions (Rydholm, 1965).

Component	% hardwood	% softwood
Lignin	22 %	29 %
Cellulose	40-50 %	40-50 %
Glucomannan & Galactoglucomannan acetate	20-35 %	12-20 %
Methylglucuronoarabinoxylan	2-5 %	10-14 %
Galactan or Arabinogalactan	1-2 %	2 %

Glucomannan, galactoglucomannan, methylglucuronoarabinoxylan, galactan, arabinogalactan and methylglucuronoxylan acetatem in Table 1 are all different types of hemicellulose. It is clear that there is no ‘best’ wood type for paper pulping, but rather that the wood used would depend on numerous factors that are specific for each plant such, as wood availability and pulping process used. The timber consumption of the Saiccor Mill consists primarily of eucalyptus hardwoods whereas Ngodwana Mills use primarily pine softwoods (Sappi, 2020).

2.3 Pulping

Pulping technology centres around the freeing the wood fibres from the wood matrix (Ek *et al*, 2009b). Pulping can be done in one of two ways, those being mechanical pulping or chemical pulping.

2.3.1 Mechanical pulping

Since Sappi utilizes chemical pulping (Sappi, 2020), mechanical pulping will not be discussed in great detail. Mechanical pulping relies on crushing and grinding wood such that the fibres are separated from the wood matrix. This gives a very high yield of between 90 % and 100 % since a very large proportion of the initial wood is grounded. Mechanical pulp fibres are normally stiff and apart from the fibres they also tend to contain a large portion of smaller material called fines. This is from fibre wall fragments and broken fibres. These give mechanical fibres unique optical properties. However, increased pulp strength is obtained if the pulp consists of a higher portion of long fibres. It has been found that mechanical pulping under higher temperatures (around 400 K) yield longer fibres and less fine formation. Because of this, chips are often pre-treated with steam.

2.3.2 Chemical pulping

The chemical way to produce pulp is to remove most of the lignin from the wood. This releases the cellulose fibres from the wood matrix (Ek *et al*, 2009b). The process of delignification relies on degrading lignin molecules and on introducing charged groups. The

lignin is dissolved into the solvent liquor and washed off during later stages. No pulping chemicals can only target lignin. Rather, the chemicals dissolve some of the carbohydrates (cellulose and hemicellulose) as well and this results in a loss of these compounds to a varying extent. Normally about half of the wood material is dissolved in chemical pulping. No chemical pulping method removes all the lignin from the pulp during pulping. Even though this would theoretically be possible, it does severely damage the carbohydrates and as such it is seldom done. The delignification is therefore ended before all lignin is removed from the pulp. The Kappa number of the pulp can be measured and this can in turn be used to estimate the residual lignin in the pulp. Ngodwana uses the T236 Tappi test, and they define the Kappa number as “the volume (in millilitres) of 0.1*N* potassium permanganate solution consumed by one gram of moisture-free pulp under specified conditions”. It does however have a straight line relationship to lignin content and therefore residual lignin content can be calculated by using the straight line equation, Equation 1 below:

$$\%Lignin = 0.13 \times \kappa \quad (1)$$

The T236 Tappi test is done at regular intervals during the day. It is a chemical analysis with oxidation. This measurement is used to calibrate the three online UV-light Kappa sensors. The three online UV-light Kappa measurement devices work by measuring the absorption of UV-light (254 μm) that has been reflection at the fiber surface of the pulp. The correlation between the UV-Kappa measurement and the Oxidation-Kappa measurement is not constant but is rather a function of the type of wood species. It is then the Sappi process engineers’ responsibility to use this correlation along with the current wood type to calibrate the UV-Kappa measurement devices to ensure minimum deviation between the online and the lab Kappa measurements.

Some chemical pulping methods include (Ek *et al*, 2009b):

Kraft cooking: It is the most popular chemical pulping method used globally. In this method, sodium hydroxide (NaOH) and sodium sulphide (Na_2S) are used as cooking chemicals to degrade the lignin molecules.

Soda cooking: Similar to the Kraft process but without sodium sulphide, using only sodium hydroxide as the active chemical.

Sulphite pulping: It utilizes sulphurous acid (H_2SO_3) and bisulphite ions (HSO_3^-) as active chemicals to degrade and dissolve lignin. In acid sulphite pulping, the pH range between 1-2 and in neutral sulphite pulping, the pH range between 7-9.

Organic solvents: Organic solvents are often used as the sole degrading chemical, as in organosolv processes. They are also commonly used as reinforcement chemical and

added to the sulphite, sulphate or soda processes. The most common solvents are ethanol (C_2H_5OH), methanol (CH_3OH) and peracetic acid ($C_2H_4O_3$).

The pulp fibres produced by chemical pulping differ from those produced by mechanical pulping. Chemical fibres are more flexible, they conform better to one another, and they offer good strength properties to the pulp. It is very common that plants which use digesters have a recovery cycle to retrieve some dissolving chemicals after the pulp has been washed. The organic component of the spent liquor (mainly dissolved lignin and hemicellulose) are then burnt in furnaces to ensure that as much as possible of the raw materials are used and waste is minimized. This is then used to create steam to heat the rest of the processes in the plant.

2.3.3 Sulphite pulping

At the Saiccor mill, DWP is produced with the use of the acid sulphite process of chemical pulping. This is a good choice of pulping method since it produces good quality DWP from the typical wood species at Saiccor (Kilian, 1999).

The main component in the cooking liquor used in the sulphite process is bisulphite (HSO_3^-), from where the process gets its name. Normally it is magnesium, calcium, sodium or ammonium that acts as the cation bonded to bisulphite. The sulphite process has some advantages over the sulphate process such as ease of pulping, higher yields of cellulose and higher cellulose content in the pulp (Gullichsen & Fogelholm, 1999).

The dissolving liquor consists of a magnesium or calcium base together with between 6 % and 7 % of dissolved sulphur dioxide (SO_2) gas and 1.2 % combined SO_2 . It is present in the cooking liquor in the form of disulphide and it corresponds to the base content of the dissolving liquor (Sandrock, 2003). The liquor composition is quantified by the total and combined SO_2 . Combined SO_2 is defined by the amount of SO_2 that is bound as neutral sulphite in the liquor (Watson, 1992). The combined SO_2 concentration is not measured directly but is rather calculated from the measured concentration of the metal oxide. During the reaction process strong acids are produced. 'Strong acids' is an umbrella term used to describe the lignosulphonic, α -hydroxysulphonic, sugar-sulphonic, sulphuric aldonic, formic, acetic and carbonic acids formed. The reaction involves the formation of anions from the complete dissociation of strong acids.

2.3.4 Sulphate (Kraft) process

At the Ngodwana mill, paper pulp is produced with the use of the sulphate process of chemical pulping. Kraft pulping is the dominant chemical pulping method worldwide (Ek *et al*, 2009b) and therefore a well-established process. Kraft pulping utilizes white

liquor, also known as strong white liquor (SWL), as the cooking liquor. It consists of sodium hydroxide, NaOH, and sodium sulphide, Na₂S, with the active cooking species being OH⁻ (measured as effective alkali(EA)) and HS⁻ (measured as sulphidity). The hydrogen sulphide serves as the main delignifying agent while the hydroxide serves to keep the lignin fragments in the solution. The name “Kraft cooking” originates from the German and Swedish word meaning “strength”. This was associated with the sulphate process that yielded paper with a high lignin content. These papers have extremely high strength. They are often used for liner-board and sack-paper because of their strength. These days, however, Kraft pulp refers to any pulp produced by the sulphate process, including bleachable grades of paper with very low lignin content.

2.3.5 Cooking procedure

The cooking procedure can take place either continuously or in batch. Both of these have their own advantages and disadvantages.

Batch process

In batch processing, a sequence of one or more steps is performed in a certain order. This yields a specific quantity of a finished product. This can take place in a single vessel or in multiple. The benefits of a batch process include (Seborg *et al*, 2011):

- Relatively small production sizes and separated batches lead to shorter response times.
- If something goes wrong with a batch, only that batch is faulty and the mistake is contained in a single batch.
- In some cases it is possible to mix batches with differing qualities to obtain the desired product quality.

Disadvantages of batch processes are:

- Downtime between batches as vessels drain or equipment needs to be cleaned or reset.
- Batch control systems are notoriously difficult.

Continuous process

Continuous processes are used to manufacture, produce or process materials without interruption. The materials, either dry bulk or fluids that are being processed, are continuously in motion, undergoing chemical reactions, heating or mechanical processes.

Continuous processes normally operate around the clock with infrequent maintenance shutdowns, such as semi-annual or annual. Advantages of continuous processing include:

- Continuous processes rarely suffer downtime. Because of this, they are usually more effective and deliver a higher yield.
- Because of the constant steady state that most continuous processes strive towards, control of continuous processes tend to be relatively simple.

Disadvantages of continuous processes are:

- Continuous processes often rely on maintaining a steady state. This sometimes lead to difficulties when there is a state that differs greatly from steady state such as startup or shut down.
- Continuous processing equipment tend to be more expensive than batch equipment, resulting in higher capital costs.

An additional challenge of continuous digesters specifically is that the operation needs to be controlled more finely than batch. If channeling occurs, for example, the liquid does not interact with the fibers, leading to high Kappa values. On the other hand, if hang ups occur at the walls or screens, this can cause overexposure to the liquid resulting in very low Kappa values. These challenges are minimal with batch digesters. It is clear from the arguments above that there is no process that is objectively the best for the use of production. The choice between batch or continuous will rely on numerous factors and some plants may opt for batch while others might opt for continuous depending on their objectives. Since continuous operation are easier to control and give better product consistency in large-scale plants, there has been a shift towards continuous digesters globally in recent years (Pikka & Andrade, 2015).

2.4 Modelling and control

In any processing plant there is an ever-increasing need to improved performance, to improve safety, to lessen environmental impact and, therefore, to tighten product quality specification. Combine this with the ever-increasing complexity and high levels of integration of processes, it becomes clear why many modern processing plants would be unable to meet all their specifications without the aid of computer based process control systems. These controllers are able to take readings and measurements from key plant variables and these are then used to manipulate other plant variables (usually flow rates by manipulation of valve positions) to ensure stable, safe and efficient operation.

2.4.1 Modelling

Most processing plants have a fairly accurate steady state model of their plant. This involves a basic mass balance of components assuming that the system will exhibit zero dynamics. This can be sufficient for very basic manual control of a simple plant, however it becomes inadequate when the system experiences large changes such as during startup or during shut down. Because of this, most plants also have a dynamic model of some sort with which they can predict the effect of large changes. This dynamic model, sometimes referred to as an unsteady state model, play an integral role in the subject of process dynamics and control. These models are used to:

- Improve the understanding of the system: Dynamic models and computer simulations (that simulate the dynamic models) of the process allow for the investigation of transient responses without causing a disturbance to production. It can also give valuable information regarding the behaviour of the process (both dynamic and steady state) even before the construction of the plant.
- Train the personnel operating the plant: Plant operators can be trained to run complex, counter-intuitive units and to deal with emergency situations by utilizing a computer simulation, rather than placing the process unit or plant at risk. The simulation can be interfaced with standard process control equipment to create a realistic training environment, making simulations a valuable asset. Running a model simulator along with process control is also often valuable as it teaches the operator about the interaction between the true plant operation and how the control system affects it. This then allows operators to understand difficult plant behaviours and they can practice dealing with them in a safe environment.
- Develop a control strategy: A dynamic model of the system allows for the evaluation of alternative control strategies. A dynamic model can help with the identification of important variables that need to be maintained or controlled and can give insight into the variables that can be manipulated to ensure that the previously mentioned variables are controlled. Dynamic models also give insight to the interactivity of the process, aiding in the choices that need to be made regarding the pairings of variables. In the event of a highly interacting system where multiple inputs affect multiple outputs (also called a MIMO system), models are often the only way to evaluate if the costs of a complex control system (such as a model predictive controller (MPC)) will be justified. For MPC control strategies, the dynamic model of the process plays an integral role in the design of the controller.
- Optimize process operating conditions: It is advised that optimum operating conditions be recalculated periodically to ensure maximum profit and minimum cost.

A process model and economic data are important tools to calculate the optimal operating conditions.

In many processes, especially when new, hazardous, complex or difficult to operate, the development of an appropriate process model can be crucial for success. There are three types of models, and they are classified based on how they are obtained. These are:

1. Theoretical models: They are obtained by using the principals of chemistry, physics and chemistry. They are often called first principal models.
2. Empirical models: They are developed by approximating a fit to experimental data.
3. Semi-empirical models: They are a combination of the two models above. The values of some parameters in a theoretical model are derive using experimental data.

Theoretical models have two great advantages. Firstly, they provide insights into the physical behaviour of the process. This can be of great value when trying to understand the process. Secondly, they are applicable over wide ranges of conditions since they use first principals. The disadvantages associated with theoretical models are that they tend to be expensive, difficult and time-consuming to develop. They also typically include model parameters that are not always readily available, such as heating coefficients and reaction rate coefficients.

Empirical models are easier to develop than theoretical models, however they come with serious disadvantages. The data set used to fit the model is typically quite small and the model is only expected to be accurate over the range covered by the model. This mean that the models don't extrapolate well and might miss notable dynamics outside the range of the data set. This could cause quite drastic prediction errors when used in operating conditions other than the ones that was used in the data set.

Semi-empirical models have three advantages. Firstly, they use theoretical knowledge. Secondly, the range of operating conditions over which they can be extrapolated is wider than that of empirical models. Thirdly, they don't require as much development effort as theoretical models do. Because of this, semi-empirical models are used to a great extent in industry.

A model of a process is nothing more than a mathematical approximation of the process. No model is perfect and no model has perfect prediction capabilities. This is because any real process has too many features (both microscopic and macroscopic) to include all of them. Because of this, no model is perfectly accurate. Modelling always involves a

compromise between the complexity and accuracy of the model, on the one hand, versus the cost and effort required to develop the model, on the other hand. This is because complex models (although generally more accurate and giving better predictions) tend to be difficult and therefore expensive to develop. On top of that, complex models often require greater computational power than more simple models, further increasing costs. A number of factors need to be considered when looking at the compromise. These include: modelling objectives, the expected benefits from model use and the intended users of the model (for example, plant engineers or research specialists). The main tool to aid in the compromise is that of simplifying assumptions. The model should display all the main dynamic behaviour, whilst at the same time, being no more complex than is needed. Because of this, less important features and phenomena are not accounted for to keep the model equations, variables and parameters to a minimum. This yields a simpler model, which is easier to work with and cheaper to design. If an inappropriate set of simplifying assumptions are chosen, the model tends to be either extremely rigorous but excessively complicated, or overly simplistic. Both of these have their own sets of disadvantages and should be avoided.

Seborg suggests a systematic approach to the development of dynamic models (Seborg *et al*, 2011):

1. Decide upon the modelling objectives and end use of the model. Decide upon the required levels of model detail and accuracy required.
2. Draw the process schematic diagram and label all variables in the process.
3. List all the model assumptions. Remember that the model should not be more complicated than necessary to meet the objective stated above.
4. Determine if spatial variations are of concern to the model. If it is the case, a partial differential equation will be necessary.
5. Write the necessary conservation equations (normally mass, energy, component, etc.). These are normally differential equations.
6. Write down equilibrium relations and other algebraic equations. These are normally from thermodynamics, chemical kinetics, equipment geometry or transport phenomena.
7. Do a Degrees of Freedom (DOF) analysis. This ensures that there are enough equations in the model to solve for all the unknowns.
8. Simplify the model. This can be done by rearranging the model equations such that the output variable is on the left side of the equation and the input variables

are on the right side. This form allows for convenient solving by computers and for easier subsequent analysis.

9. Classify the inputs to the model as either disturbances variables or manipulated inputs. In general, disturbance variables are determined by the environment or by other process units.

To simulate a process, it needs to be ensured that the model equations (both differential and algebraic) together constitutes a set of relations that can be solved. This means that all the output variables can be solved in terms of the input variables. For example, take $y = Ax$, a set of linear equations. For x to have a unique solution, vectors x and y must contain the same number of elements. Also, matrix A needs to be non-singular (it should have a nonzero determinant). It is not always easy to make a similar evaluation for large and complex models, however, one rule needs to be obeyed. Only if the number of unknown variables are equal to the number of independent model equations, can the model have a unique solution. This is to say that all the available degrees of freedom are utilized. The number of degrees of freedom (N_F) are given by Equation 2 below:

$$N_F = N_V - N_E \quad (2)$$

With N_V being the total number of process variables and N_E the number of independent model equations. This means that the degrees of freedom of a system can either be equal to, greater than, or less than zero. In the event that:

- $N_F = 0$, the number of model equations is equal to the number of process variables. The set of equations will have a solution and the process model is exactly specified.
- $N_F > 0$, there are more process variables than there are equations. This means that the independent equations have an infinite number of solutions. This is because the degrees of freedom process variables can arbitrarily be specified. The process is underspecified.
- $N_F < 0$, There are fewer process variables than equations and because of that the set of equations does not have a solution. The process model is over specified.

The only satisfactory case is the exactly specified model. If the process is underspecified, a sufficient number of input variables need to be assigned numerical values. If the process is over specified, additional independent model equations should be developed if the model is to have an exact solution. The steps taken to analyse the degrees of freedom are listed below:

1. All known constants or parameters in the model are listed. These values are obtained from equipment dimensions, known physical properties etc.

2. Determine the number of process variables as well as the number of independent process equations. Note that t denoting time is not included since it's neither a process input, nor process output.
3. Calculate the degrees of freedom using Equation 2
4. Identify the number of equation output variables that will result from solving the process model. This includes the dependant variables from the ordinary differential equations.
5. Determine the number remaining variables that should be specified as disturbance and manipulated variables, to achieve zero degrees of freedom.

Once a model is exactly specified, it can be evaluated and further expanded on if deemed inaccurate or too complicated. The model however, should be solvable if and only if it is exactly specified.

2.4.2 Batch models vs continuous models

It is often thought that batch process models and continuous process models are very similar, with both having a dynamic element and, in the majority of cases, some non-linear equations as well (Kilian, 1999). One of the main differences however, is that continuous models work around a single steady state value, whereas a batch process normally has a much wider range of operation. Because of this, continuous models tend to concentrate a lot of attention on a fairly small area, whereas, batch process models are a lot more rigorous to equip them for prediction over the whole range of conditions encountered. These process conditions may vary wildly from the beginning of the process to the end (Rippen, 1982). Even though continuous process models tend to focus on smaller ranges of operation, the penalties for inaccurate predictions are usually higher in a continuous plant than in a batch plant.

2.5 UP model

At Saiccor, Sappi uses batch digesters to produce DWP. They have 23 synchronized batch digesters.

Kilian (1999) developed the preliminary UP model for the batch digesters at Saiccor from first principals. These parameters, that the model uses, are optimized to fit data obtained experimentally from the plant. The assumptions of the model are (Sandrock, 2003):

1. The components accounted for are cellulose, hemicellulose, lignin and strong acids.
2. The pressure and temperature of the digester are known at discrete times.

3. The conditions of the system initially are determined by analysing a liquor sample.

The kinetics of the cellulose is emphasized since the quality of the product is based on its quality. The temperature and pressure in the reactor affects the equilibrium state of SO_2 , which, in turn, affects the composition of the cooking liquor (Stephens, 2017).

2.5.1 Reaction rates

The UP model is modelled after a batch reactor. It is therefore modelled under the assumption of constant volume. Under this assumption, the rate of change of concentration is given by Equation 3 (Levenspiel, 1999).

$$r_i = \frac{1}{V} \frac{dN_i}{dt} \quad (3)$$

Numerous studies have been done on acid pulping. The reaction kinetics suggested by Hagberg & Schöön (1973) are used in this model. The kinetic parameters of the rate equation are reliant on the process conditions and the properties of the wood. Because of this, the parameters are adapted regularly to accurately model the plant. The kinetic equations that describe lignin dissolution, cellulose degradation, hemicellulose degradation and strong acid formation are given below.

$$-\frac{d[L]}{dt} = k_L [L]^a [\text{HSO}_3^-]^\alpha [\text{H}^+]^\beta \quad (4)$$

$$-\frac{d[C]}{dt} = k_C [\text{H}^+]^\delta \quad (5)$$

$$\frac{d[HC]}{dt} = k_{HC} [HC]^d [\text{H}^+]^\gamma \quad (6)$$

$$\frac{d[\text{SA}^-]}{dt} = \left\{ \left(\frac{g}{\nu} + \frac{2h}{\nu} \right) ([L]_0 - [L]) \right\} r_L + \frac{k_{SA}(T)}{\nu} ([L]_0 - [L])^q [\text{HSO}_3^-]^b [\text{H}^+]^c \quad (7)$$

In the original model the concentration of hemicellulose was calculated using Equation 6, however, in the current model, the degradation rate of hemicellulose is implicitly calculated in these equations above (de Vaal & Sandrock, 2007). The rate constants (k_i) used in Equation 4-7 above are known to have a temperature dependence. They follow the Arrhenius equations given by Equation 8-11 below: (Hagberg & Schöön, 1973)

$$k_L = k_L^0 \exp\left(\frac{-E_a^L}{RT}\right) \quad (8)$$

$$k_C = k_C^0 \exp\left(\frac{-E_a^C}{RT}\right) \quad (9)$$

$$k_{HC} = k_{HC}^0 \exp\left(\frac{-E_a^{HC}}{RT}\right) \quad (10)$$

$$k_{SA} = k_{SA}^0 \exp\left(\frac{-E_a^{SA}}{RT}\right) \quad (11)$$

Since both E_a and R are constants, the expression $\frac{-E_a}{RT}$ is sometimes written as $\frac{-E}{T}$. Important assumptions regarding the kinetics of the system are:

1. It would be close to impossible to describe a different reaction rate equation for every different type of lignin and hemicellulose. Therefore, even though lignin and hemicellulose are both collective nouns for numerous similar compounds, their reactions will be treated as single degradation reactions.
2. The concentration of the reactants inside the wood chip will be assumed to be the same as the concentration of the reactants in the bulk liquor. The rate of diffusion into and out of the chip is therefore assumed to be negligible. It is known that the diffusion path is very short once the cooking liquor completely penetrated the wood chip (Kilian, 1999).
3. The digester was divided into 10 volumes to calculate the temperature gradient. Ideal mixing of each these volumes is assumed.
4. The heat of reaction of the degradation reactions are assumed to be negligible in the temperature calculations of the digester. This is because literature on this is hard to come by and the heat of reaction seems to be small in comparison to the energy required to heat the digester. It seems that the exothermic reactions do little to heat up the digester.

2.5.2 Liquor composition

It is clear that all the reaction rate equations (Equations 4-7) are dependent on the concentration of hydrogen ions. Because of this, the liquor composition needs to be modelled. It is modelled using the equilibrium equations for the SO_2 concentration in the liquor as well as the vapour pressure of the volume above the liquor. This yields Equations 12 and 13 below.

$$K_{\text{SO}_{2f}} = \frac{[\text{H}^+][\text{HSO}_3^-]}{[\text{SO}_{2f}]} \quad (12)$$

$$K_P = \frac{[\text{H}^+][\text{HSO}_3^-]}{p_{\text{SO}_{2f}}} \quad (13)$$

Both $K_{\text{SO}_{2f}}$ and K_P are temperature dependant. They can be calculated by using the Antoine equation and this is described by Equations 14 and 15

$$\log_{10} K_{\text{SO}_{2f}} = B_{\text{SO}_{2f}} + \frac{C_{\text{SO}_{2f}}}{T} \quad (14)$$

$$\log_{10} K_p = B_p + \frac{C_p}{T} \quad (15)$$

The metal ion concentration in the batch is to be modelled by using electron-neutrality arguments as described in Equations 16 and 17 below:

$$[M^+] + [H^+] = [HSO_3^-] + [SA^-] \quad (16)$$

$$[M^+] = 2[SO_{2f}C] \quad (17)$$

Where $SO_{2f}C$ denotes the combined free SO_2 concentration. Assuming that the volume above the liquor in the batch consist of only water vapour and SO_2 , the total pressure of the digester can be determined by summing the partial pressures of the components in the vapour phase. This is shown in Equation 18 below.

$$P = p_{SO_{2f}} + p_{H_2O_f} \quad (18)$$

Table 2: Variables used by the UP model.

Symbol	Description	Unit
$[L]$	Residual Lignin concentration	mass %
$[C]$	Cellulose concentration	$\frac{kmol}{m^3}$
$[HSO_3^-]$	Sulfite concentration	$\frac{kmol}{m^3}$
$[H^+]$	Hydrogen ion concentration	$\frac{kmol}{m^3}$
$[SA]$	Strong acid concentration	$\frac{kmol}{m^3}$
T	Temperature	K
P	Pressure	Pa_a
p_{SO_2}	Partial pressure of SO_2	Pa
p_{H_2O}	Partial pressure of water	Pa
K_{SO_2}	Dilution constant of SO_2	$\frac{kmol}{m^3}$
K_P	Vapour-liquid equilibrium constant	$\frac{kmol}{m^3} / Pa$
SO_{2C}	Combined SO_2	$\frac{kmol}{m^3}$
SO_{2f}	Free SO_2	$\frac{kmol}{m^3}$
$[M^+]$	Total positive charge	$\frac{kmol}{m^3}$
ν	Specific volume of liquor	m^3
E_a	Activation energy	$\frac{J}{mol}$
R	Universal gas constant	$\frac{J}{molK}$

It is clear from the model that there are 18 variables and 13 equations. These 18 variables are the first 15 variables in Table 2 along with the three rate constants (k_L , k_C and k_{SA}). The 13 equations are Equations 4 to 18, omitting Equations 6 and 10 since the degradation rate of hemicellulose is implicitly calculated in these equations above in the

current model (de Vaal & Sandrock, 2007). Therefore, 5 additional variables need to be specified to completely specify the system. The 5 input variables are: the temperature and pressure from the cook, the liquor-to-wood ratio, and the free and combined SO₂ concentrations. The cook temperature and pressure are read from the measurements during the cook while the liquor-to-wood ratio is known at the start of the process and the free and combined SO₂ concentrations are obtained at the start of the cook during the 1-h test (de Vaal & Sandrock, 2007). Specifying these five variables as inputs completely specifies the problem.

It should be noted that the reaction kinetics of a digester are very complex, with a multitude of reagents reacting differently, creating various substances. These models (the UP model and the rest that will be discussed) were therefore developed by empirically fitting equations to measurements that were made. This gave the reaction kinetics. Although they are all thoroughly studied and predict the reactions well, they are not first principal models with chemistry in mind. This means that, although the reaction kinetics predict the main wood components well, the model does not predict the rate of reaction of all the byproducts that form. These include but are not limited to what you mentioned namely: liquefied organic compounds, Na₂CO₃ and Na₂SO₄. These models do not have equations for the byproducts and will therefore not be able to track their concentrations. If they are deemed important enough, they can be added to the model, although some experimentation might be needed to determine these lesser reaction kinetics.

2.6 Continuous model history

There exists an extensive history of digester modelling. This is because it is such a difficult process to accurately model and it has many factors that can be accounted for. The first proposed model for a continuous digester is the Purdue model.

2.6.1 Groundwork of the Purdue model

The foundation work of continuous Kraft digester modelling was done by Smith & Williams (1974). They developed the well-known Purdue model (so called as it was developed at the Purdue University). They developed kinetic models to describe the delignification process. Their models have the form:

$$R_{s,i} = -[k_{1,i}(T)C_{OH}^a + k_{2,i}(T)C_{OH}^b C_{HS}^c](C_{s,i} - C_{s,i}^\infty) \quad (19)$$

with the temperature dependant rate constants determined using the Arrhenius law:

$$k_{i,j}(T) = A_{i,j} \exp\left(\frac{-E_{i,j}}{RT}\right) \quad (20)$$

They described wood as consisting of 5 parts. These are high reactive lignin (s_1), low reactive lignin (s_2), cellulose (s_3), galactoglucomannan (s_4), and araboxytan (s_5). The last 2 account for hemicellulose. Index i refer to the 2 rate constants while index j refer to the 5 solid components in the chips. From there, model constants ($a, b, c, A_{i,j}, E_{i,j}$) were evaluated by trial and error with the aid of pulping chemistry data. They approximated the digester as a series of continuously stirred tank reactors (CSTRs). With this they could obtain dynamic mass balances for each of the main components in the pulping reactions. There are 3 phases assumed to be contained in each of these CSTRs, namely:

1. The solid phase consisting of the solid wood.
2. The entrapped liquor phase consisting of the liquor in the pores of the wood.
3. The bulk free liquor phase consisting of the free liquor surrounding the wood chips.

This model formed the framework for numerous other models to follow.

2.6.2 Further innovation

One of the first to follow was the model of Christensen *et al* (1982). They improved the kinetic parameters by using an optimization search. This increased the validity of the model over a larger range of wood species. The new model predicted blow-line Kappa numbers as well as free liquor concentration profiles, both being important for quality control.

Gustafson *et al* (1983) described the delignification reaction by developing alternate kinetic expressions. These expressions use fewer wood and liquor components. It utilizes the functional relationship between cellulose and lignin consumption rate. Greater attention is paid to liquor penetration into the wood chips.

Kayihan *et al* (1996) developed a Weyerhaeuser benchmark model for a Kamyr (Kraft) digester that has two vessels, one for impregnation of steam and one for the reaction. The Weyerhaeuser Benchmark Digester Problem is a simplified digester model, which captures the main characteristics of a continuous digester. The model assumes two phases (non-porous solids and free liquor) in thermal equilibrium. This differs from the 3 phases used by Smith & Williams (1974). The kinetic model uses an adaptation of the work done by Christensen *et al* (1982) to describe dynamic mass balances.

Wisniewski, Doyle & Kayihan (1997) redefined the mass concentrations and volume fractions. This allowed for some relaxation in the Purdue model assumptions, which increased the reliability of the model. This model compared well to the original Purdue model,

capturing the same range of behaviours. It also compared well to the Weyenhaeuser benchmark model, capturing the same range of behaviours.

All the models discussed so far neglect to account for a change in chip density throughout the column. They all assume an unchanging compaction profile and none of them provide a dynamic description of the chip level. This is because the momentum balance has been neglected.

Härkönen (1987) was one of the first to give a hydraulic description of a continuous digester. This entailed a detailed description of the compaction as well as the chip and liquor flow dynamics in addition to mass and energy transports. His work laid the foundation for the integration of digester hydraulics with existing models that were based on mass and energy transport.

Michelsen (1995) proposed the integration of the work by Christensen *et al* (1982) and Härkönen (1987) to result in a model with mass, energy and transport balances. The work by Bhartiya, Dufour & Doyle (2003) then integrated the work of Michelsen (1995) and Wisniewski *et al* (1997) to yield a detailed model giving the best results of both models.

2.7 Kraft model

Since it is the aim to adapt the UP model to accommodate the dynamics and kinetics of a continuous Kraft pulping process, it was decided to take a look into an existing Kraft model to be able to compare models. The model by Christensen *et al* (1982) was chosen as it gives a reasonable model of the kinetics without being too complex. The aim is mainly to compare the models to see where differences exist. This model by Christensen *et al* (1982) will therefore be discussed below.

The kinetic equations used are given as:

$$\frac{dL_1}{dt} = -[k_1(OH) + k_2(OH)^{0.5}(HS)^{0.5}] \times L_1 \quad (21)$$

$$\frac{dL_2}{dt} = -[k_3(OH) + k_4(OH)^{0.5}(HS)^{0.5}] \times L_2 \quad (22)$$

$$\frac{dC_1}{dt} = -[k_5(OH) + k_6(OH)^{0.5}(HS)^{0.5}] \times (C_1 - C_{1U}) \quad (23)$$

$$\frac{dC_2}{dt} = -[k_7(OH) + k_8(OH)^{0.5}(HS)^{0.5}] \times (C_2 - C_{2U}) \quad (24)$$

$$\frac{dC_3}{dt} = -[k_9(OH) + k_{10}(OH)^{0.5}(HS)^{0.5}] \times C_3 \quad (25)$$

C_{1U} and C_{2U} refer to unreactive cellulose and unreactive galactoglucomannan respectively. Christensen *et al*, 1982 suggests that around 70% of cellulose and around 25% of galactoglucomannan may be unreactive. Reasons for this include that some of the galactoglucomannan and cellulose do not possess aldehydes as end groups, meaning that they are not easily attacked by the hot alkali. Other cellulose and galactoglucomannan seem to be protected from the hot alkali by the wood morphology. Lastly the pulping process may result in carboxylic end groups on the cellulose and galactoglucomannan, which are also alkali stable. Because of this the unreactive components are included in the model.

The rate of change in concentration of hydroxide and hydrosulphide in the entrapped liquor can be given by the equations below:

$$\frac{d(OH)}{dt} = \frac{1}{V_e} \left[KA((OH)_f - (OH)) + (b_{COHL} - 0.5 \times b_{CSHL}) \times \left(\frac{dL}{dt} + b_{COHC} \times \frac{dC}{dt} \right) \right] \quad (26)$$

$$\frac{d(HS)}{dt} = \frac{1}{V_e} \left[KA((HS)_f - (HS)) + 0.5 \times b_{CSHL} \times \left(\frac{dL}{dt} \right) \right] \quad (27)$$

with:

$$KA = \begin{cases} 3.8 \times 10^{-5}(T_c - 273) - 1.1 \times 10^{-3} & T_c \leq 373K \\ 6.6 \times 10^{-5}(T_c - 273) - 3.9 \times 10^{-3} & 373K \leq T_c \leq 423K \\ 1.2 \times 10^{-4}(T_c - 273) - 1.2 \times 10^{-2} & 423K \leq T_c \end{cases} \quad (28)$$

The accumulation of dissolved solids (X) in the entrapped liquor is given by:

$$\frac{dX}{dt} = \frac{1}{V_e} \left[KA(X_f - X) - \frac{dW}{dt} \right] \quad (29)$$

With W as the total wood mass. The rate of change in concentration of hydroxide, hydrosulphide and dissolved solids in the free liquor is, in turn, related to rate of diffusion as follows:

$$\frac{d(OH)_f}{dt} = -\frac{KA}{V_f} [(OH)_f - (OH)] \quad (30)$$

$$\frac{d(HS)_f}{dt} = -\frac{KA}{V_f} [(HS)_f - (HS)] \quad (31)$$

$$\frac{d(X_f)}{dt} = -\frac{KA}{V_f} [X_f - X] \quad (32)$$

The variables used in the model above will be detailed in Table 3 below:

Table 3: Christensen, Albright & Williams (1982) model variables.

Variable	Description	type	Units
L_1	high reactivity type lignin	Input	$\frac{\text{kg}}{\text{kg}_{ODW}}$
L_2	low reactivity type lignin	Input	$\frac{\text{kg}}{\text{kg}_{ODW}}$
C_1	cellulose	Input	$\frac{\text{kg}}{\text{kg}_{ODW}}$
C_2	galactoglucomannan	Input	$\frac{\text{kg}}{\text{kg}_{ODW}}$
C_3	araboxylan	Input	$\frac{\text{kg}}{\text{kg}_{ODW}}$
C_{1U}	unreactive cellulose	Parameter	$\frac{\text{kg}}{\text{kg}_{ODW}}$
C_{2U}	unreactive galactoglucomannan	Parameter	$\frac{\text{kg}}{\text{kg}_{ODW}}$
OH	entrapped hydroxide concentration	Input	$\frac{\text{kg}}{\text{m}^3}$
HS	entrapped hydrosulphide concentration	Input	$\frac{\text{kg}}{\text{m}^3}$
k_i	$A_i e^{-\Delta E_i / RT}$	Output	
A_i	frequency factor	Input	$\frac{\text{m}^3 \text{h}}{\text{kg}}$
ΔE_i	activation energy	Parameter	kJ
R	universal gas constant	Parameter	$\frac{\text{kJ}}{\text{molK}}$
T	temperature	Input	K
$\frac{dL}{dt}$	$\frac{dL_1}{dt} + \frac{dL_2}{dt}$	Output	$\frac{\text{kg}}{\text{h}}$
$\frac{dC}{dt}$	$\frac{dC_1}{dt} + \frac{dC_2}{dt} + \frac{dC_3}{dt}$	Output	$\frac{\text{kg}}{\text{h}}$
KA	mass transfer coefficient \times area	Output	$\frac{\text{m}^3 \text{h}}{\text{kg}}$
OH_f	hydroxide concentration of free liquor	Input	$\frac{\text{kg}_{NaOH}}{\text{m}^3}$
HS_f	hydrosulphide concentration of free liquor	Input	$\frac{\text{kg}_{NaOH}}{\text{m}^3}$
b_{COHL}	OH consumption by lignin	Parameter	$\frac{\text{kg}_{NaOH}}{\text{kg}_{lignin}}$
b_{CSHL}	consumption of HS by lignin	Parameter	$\frac{\text{kg}_{NaOH}}{\text{kg}_{lignin}}$
b_{COHC}	OH consumption by carbohydrates	Parameter	$\frac{\text{kg}_{NaOH}}{\text{kg}_{carb}}$
X	dissolved solids in the entrapped liquor	Input	$\frac{\text{kg}}{\text{m}^3}$
X_f	dissolved solids in the free liquor	Input	$\frac{\text{kg}}{\text{m}^3}$
$\frac{dW}{dt}$	$\frac{dL}{dt} + \frac{dC}{dt}$	Output	$\frac{\text{kg}}{\text{h}}$
V_e	Entrapped volume	Output	m^3
V_f	Free volume	Output	m^3
ρ	liquid density	Parameter	$\frac{\text{kg}}{\text{m}^3}$
m_{crit}	Critical moisture content	Parameter	$\frac{\text{kg}_{water}}{\text{kg}_w}$
LtW	Liquor to wood ratio	Parameter	$\frac{\text{kg}_l}{\text{kg}_w}$

The initial conditions for Equations 21 to 25 are lignin-, cellulose, galactoglucoaraannan and araboxylan in wood, as follows

$$L_1(0) = 0.2 \times (L) \quad (33)$$

$$L_2(0) = 0.8 \times (L) \quad (34)$$

$$C_1(0) = C \quad (35)$$

$$C_2(0) = H_1 \quad (36)$$

$$C_3(0) = H_2 \quad (37)$$

with L being the lignin content of the wood, C the cellulose content of the wood, H_1 the galactoglucoraannan content of the wood and H_2 the araboxyylan content of the wood. All of L , C , H_1 , H_2 , $L_1(0)$, $L_2(0)$, $C_1(0)$, $C_2(0)$ and $C_3(0)$ have units of $\frac{\text{kg}}{\text{kg}_{ODW}}$. The model is now fully defined and ready to be compared to the UP model. As with the UP model it should be noted that the reaction kinetics were developed by empirically fitting equations to measurements that were made. They all predict the reactions well, although they are not first principal models with chemistry in mind. The reaction kinetics predict the main wood components well but the model does not predict the rate of reaction of all the byproducts that form. the model does not have equations for the byproducts and will therefore not be able to track their concentrations. If they are deemed important enough, they can be added to the model, although some experimentation might be needed to determine these lesser reaction kinetics.

2.8 Method of lines as a partial derivative solution technique

First principle models of the physical world are generally described with respect to both time and three-dimensional space. These descriptions are often times translated into mathematics with the use of partial differential equations (PDEs) (Schiesser & Griffiths, 2009).

2.8.1 Partial differential equations

A PDE is any type of differential equation with two or more independent variables. Differential equations with a single independent variable is simply an ordinary differential equation (ODE) and these can be easily solved numerically with the use of Euler integration or more sophisticated numerical integration techniques that are widely available in various software libraries and packages. The independent variables of a PDE can be divided into two categories. They are either defined as an initial-value variable or a boundary-value variable. In cases where physical systems are concerned, time (t) is termed the initial-value variable. Since it starts at an initial value (t_0), it is an initial-value variable. It then moves forward over either a finite interval ($t_0 \leq t \leq t_f$) or a semi-infinite interval ($t_0 \leq t \leq \infty$) without any further imposed conditions. The rest of the variables (usual related to space, such as x , y , z position or combination thereof) are then termed boundary-value variables. The boundary-value variables either vary over

a finite interval ($x_0 \leq x \leq x_f$ with x being a boundary-value variable), a semi-infinite interval ($x_0 \leq x \leq \infty$) or a fully infinite interval ($-\infty \leq x \leq \infty$) and at one or more values of x depending on the order of the PDE in terms of x , conditions are imposed on the output. Normally, the values of x relate to physical boundaries of a system and from this derives its name (Schiesser & Griffiths, 2009).

When looking at solving a PDE, one can look to solve it either numerically or analytically. Although the analytical solution would be powerful, the numerical solution is normally easier and therefore quicker to determine and for the purposes of system modelling the numerical solution is normally sufficient. One of the possible ways to go about solving a PDE numerically is to use the method of lines (MOL).

2.8.2 Method of lines

The main point of the MOL is to replace the boundary-value (spatial) variables and derivatives with algebraic approximations in the PDE. After this, these derivatives are not explicitly stated in terms of the spatial independent variables any more. Therefore, upon rewriting, only the initial-value variable (time normally) remains and the PDE has been simplified and approximated as an ordinary differential equation (ODE). The challenge lies in formulating this system of ODEs that approximate the PDE. Once the system has been reduced to a system of ODEs, any integration algorithm for initial value ODEs can be used to calculate the approximate numerical solution to the original ODE. This is one of the advantages of the MOL, as it allows for the use of existing and well-established numerical ODE solving methods (Schiesser & Griffiths, 2009).

2.9 State estimation

Since the purpose of a model is to simulate the state of a system, it is essential to have as much knowledge of the system's state as possible. Sometimes these states are closely measured, however, more likely than not, only noisy measurements will be available if anything. Ideally the entire state would be measured but in most industrially relevant cases, only a subset of the system states are measured. All models however, rely on initial value conditions and if these conditions are not accurate the model might also be inaccurate. Because of this, it is vital to be able to reconstruct the states of a system using noisy measurements. Perhaps the most famous system state estimation method is the Kalman filter. It is the statistically optimal state estimator for linear systems with normally distributed disturbances and noises. Also, because of its linear nature, it is quite fast and efficient. In general there are two approaches to non-linear state estimation. These are to use the modified Kalman filter or the moving horizon estimation. These will be discussed below:

2.9.1 Modified Kalman filters

The modified Kalman filter entails first designing an observer (a parallel dynamic system) that takes the outputs of the original system as its inputs and then produces, as output, an estimate of the state of the original system. Two popular observers are the extended Kalman filter (EKF) and the unscented Kalman filter (UKF). The EKF's state consists of an estimate of the actual state of the system, as well as, the estimate's state covariance matrix (Rakovic & Levine, 2018). Using the non-linear model, the estimated state is propagated forward in time. The estimate is then corrected by linearizing the non-linear model at the estimated state and by applying the Kalman filter equations to the covariance matrix. This is easy and quick to implement but is only reliable of systems that are nearly linear. The UKF on the other hand, is an observer that takes an ensemble of states close to the estimated state. It runs the ensemble through the non-linear system model, and the result statistics of the ensemble are then used for the state update. This approach is normally better and more accurate on systems with highly non-linear dynamics or measurements than the EKF.

2.9.2 Moving horizon estimation

The second approach takes the non-linear process model and optimizes over it to find the state trajectory that would most likely have caused the measured outputs. In other words, the Moving horizon estimation (MHE) forecasts the behaviour of the system with the use of a non-linear model over a certain time horizon, based on the initial estimate of the system of the state. It then optimizes to find the smallest disturbances to this prediction that is necessary to account for the data of the measurements. This is illustrated, to some extent, in Figure 1 below:

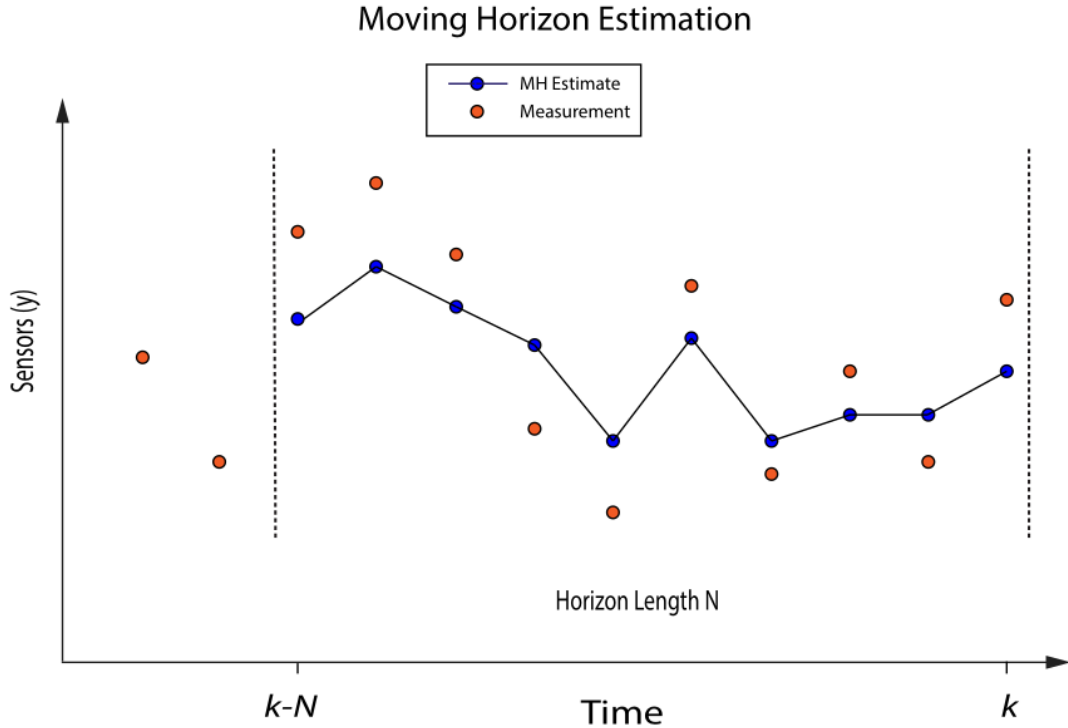


Figure 1: Moving horizon estimation using a system model and optimization to reconcile past measurements over a horizon of length N .

Normally two disturbances are considered, these being firstly the state disturbances and secondly, the measurement disturbances. The state disturbances have a direct impact on the state of the system, and, because of this, their effects propagate through the system. The measurement disturbances however, appear to affect the state of the system without altering it in reality. Because of this, their effect does not propagate through the system. The stage cost of the estimator (or the optimization cost function), dictates the likelihood of any one disturbance occurring. So, for example, a weighted least squares cost function implies that numerous small disturbances are more likely than fewer larger disturbances, whereas an ℓ_1 cost function implies that many small disturbances are just as likely as fewer larger disturbances. The quadratic stage cost is the most popular, because of its ties with the Gaussian distribution of disturbances. The initial conditions (or prior) is taken into account with the use of a prior weighting. This prior is almost always incorrect and, because of that, it is important to be able to move it such that it can predict a stage trajectory that is most aligned with the measurements observed. Without any prior weighting, the system must be observable for the estimator to converge to an answer. A system is observable if its system state can be reconstructed using a finite number of measurements. Decent prior weighting is therefore very important for good MHE performance. The objective function (V_N) is typically given in the form of

Equation 38 below (Rakovic & Levine, 2018):

$$V_N(\chi, \omega, \nu, \bar{x}) := \rho V_p(\chi, \bar{x}) + \sum_{k=0}^{N-1} \ell(\omega(k), \nu(k)) \quad (38)$$

with χ denoting the predicted initial state, ω the measured system output, ν the predicted system output, \bar{x} the initial states, ρ a constant chosen larger than 0 to ensure robust stability, V_p the prior weighting, k the time of estimation, N the estimation horizon, and ℓ the state function (weighted least square, ℓ_1 , etc.). With this, an estimate for the states of the system can be determined. The weighting functions also allows for decisions regarding the likelihood of initial states being close to correct.

2.9.3 Comparison of state estimators

As mentioned previously, it is known that the UKF usually outperforms the EKF (except in cases of near linearity). The comparison between the performance of the EKF and the MHE was done by Haseltine & Rawlings (2005) and it was found that the MHE consistently yielded better state estimation and improved robustness to poor initial guesses as well as tuning parameters when compared to the EKF. This comes at the cost of greater computational expense required to solve the MHE optimization. The comparison between the performance of the UKF (and the ensemble Kalman filter — both being Bayesian state estimation algorithms) and the MHE was done by Bavdekar, Gopaluni & Shah (2013) and it was found that the use of MHE resulted in better state estimation when compared to these recursive Bayesian state estimators. They did add however, that the MHE does not help to compensate for model plant mismatch. These findings are also yielded by Varshney *et al* (2019) who compared both EKF and UKF to MHE.

2.10 Adaptive control

As a system is simulated, it is normal for some assumed parameters to drift over time. A solution to this is adaptive control, which will be discussed below:

2.10.1 Parameter drift

Any model of a physical system is likely to utilize some parameters. These parameters can be specific to the system (such as the volume of a tank or the heat transfer area of a pipe), or these can be universal parameters (such as the universal gas constant or the activation energy required for a given chemical reaction). Often, however, it happens that a variable that is fairly constant over time is labelled as a parameter, normally either to simplify the model or because the variable is not measured. This can include variables such as ambient temperature, heat transfer coefficient of vessel, ratios of chemicals in

feed, flow rates, feed composition, heat capacity of a mixture etc. In the above examples however, the ambient temperature is not constant and changes dramatically as seasons change in some areas of the world. The heat transfer coefficient of a vessel tends to change over time if there is fouling, scaling, corrosion or coking present in the vessel. Chemical feed ratios as well as feed flow rates (if considered a parameter) are normally fixed with the use of a controller. This, however does not mean that the value remains constant throughout operation and the value will tend to vary slightly with time. In some cases, especially for the wood pulping industry, the assumption is made that the feed (e.g. wood) composition remains constant. The composition of any natural material is a function of various environmental variables and might also change over time. The heat capacity of mixtures also change as the composition of the mixture changes and, although the effect on the heat capacity of the mixture might be small, it still changes with time. This can potentially be a modelling challenge and can lead to model inaccuracy if not correctly accounted for.

2.10.2 Parameter optimization

A solution to this is to use adaptive control and, in this case, it will consist of periodically optimizing the system parameters (VanDoren, 2003). This means that every so often (perhaps once every month or 3 depending on the speed of parameter change), the model will look back at the last few data points (more data points should lead to increased accuracy but increased computational time). If MHE is employed, it is advised to implement it from all the data points between the current time and the time of the implementation of the MHE. Using these data points, it will then re-simulate the last data points. During these re-simulations, certain pre-determined parameters will be varied. This will then be fed to an optimization function that will compare the resulting outputs to that of the observed data. Optimizing the parameters using the optimization function will then yield the parameters such that the results most closely follow the data. This can then be used to reset parameters to more adventitious values.

3 Model decision

Various models can be employed to aid in creating the digester model. These include the models by Christensen *et al* (1982), Bhartiya *et al* (2003), the UP model or starting from first principles. This is an important decision that will decide the ultimate course of the project.

3.1 Preface

The UP model was developed by the University of Pretoria and a lot of research has gone into its development. Therefore, it would be advantageous to be able to adapt if further for the modelling of continuous digesters. The UP model has proved successful for the sulphite process at Saiccor (Stephens, 2017), however, the digester at Ngodwana operates using the sulphate (Kraft) process. With differing active ingredients, not only the reaction parameters but also the dependence of reaction rate on concentrations will change. Another difference is that Saiccor uses hardwoods whereas Ngodwana uses softwoods. This, however, should only influence some model parameters. Besides this, there are also numerous digester specific parameters that are going to be different such as volume of the digester and so forth. This is to be expected and should not present a challenge. Because of all this, the UP model might not be able to adequately predict the reaction kinetics of the digester. To solve this potential problem, it was decided to compare the UP model against a Kraft process model to see if the equations (and specifically the reaction kinetics) are similar enough that the UP model can be deployed. The Kraft process model chosen was the model by Christensen *et al* (1982). This model was chosen because it is fairly detailed with an emphasis on the kinetics of the model. However, even though it is fairly detailed, it is not as complex as the model of Bhartiya *et al* (2003) for example. It is still simple enough to use as a first comparison to the UP model.

3.2 Model comparison

Both of these models consist mainly of reaction kinetic equations for both the wood components and the liquor reagents. The wood component reaction kinetics will be compared first below.

UP model

The UP model only distinguishes between 3 wood components (lignin, cellulose and galactoglucomannan, araboxylan). The reaction rate equations (Equations 4 to 6) are given below.

$$-\frac{d[L]}{dt} = k_L[L]^{\alpha}[\text{HSO}_3^-]^{\alpha}[\text{H}^+]^{\beta}$$

$$-\frac{d[C]}{dt} = k_C[H^+]^\delta$$

$$\frac{d[HC]}{dt} = k_{HC}[HC]^d[H^+]^\gamma$$

Kraft model

The Kraft model distinguishes between 5 wood components (fast reacting lignin, slow reacting lignin, cellulose and hemicellulose). The reaction rate equations (Equations 21 to 25) are given below.

$$\frac{dL_1}{dt} = -[k_1(OH) + k_2(OH)^{0.5}(HS)^{0.5}] \times L_1$$

$$\frac{dL_2}{dt} = -[k_3(OH) + k_4(OH)^{0.5}(HS)^{0.5}] \times L_2$$

$$\frac{dC_1}{dt} = -[k_5(OH) + k_6(OH)^{0.5}(HS)^{0.5}] \times (C_1 - C_{1U})$$

$$\frac{dC_2}{dt} = -[k_7(OH) + k_8(OH)^{0.5}(HS)^{0.5}] \times (C_2 - C_{2U})$$

$$\frac{dC_3}{dt} = -[k_9(OH) + k_{10}(OH)^{0.5}(HS)^{0.5}] \times C_3$$

Discussion

If the UP model would be adapted for use on the Kraft model, the reacting liquor components would be substituted for the reagents in the Kraft process. Along with this, parameters for the reaction kinetics will be optimized against plant data since the reaction rate parameters will be different for differing reagents. For this to be done however, it is important that the reaction rate equations be similar enough in form that a transformation can be made. From the equations above however, it is clear that there are some large differences. These include the UP model cellulose differential equation that is not a function of cellulose concentration whereas the Kraft model is, as well as the differential equations for cellulose and hemicellulose in the UP model being only a function of one reagent whereas, in the Kraft model it is a function of both reagents. These differences were decided to be large enough to discount the option of using the UP model to model the Kraft process.

3.3 Kraft model selection

After eliminating the UP model, the only options remaining were to either develop a model from first principles without regarding previous work done or to choose and adapt an already existing Kraft model from literature. Because of the added difficulty and with no desire to ‘reinvent the wheel’, it was decided to look to the literature to identify a

model that can be adapted to suit the needs of the model. As discussed in Section 2.6, there are numerous Kraft process models that can be chosen from when looking to adapt the model. It was then decided that the Purdue model (Smith & Williams, 1974) was as simple as it came and that, although simplicity would be advantageous, it was decided to rather opt for a slightly more advanced model. The optimal mix of complexity and function was reached with the model by Christensen *et al* (1982). It is more advanced than the Purdue model, yet not as complicated as the models by Wisnewski *et al* (1997), Bhartiya *et al* (2003) or Michelsen (1995) for example. Also, there is an emphasis on reaction kinetics instead of hydraulics, which also suited the desired outcome. Lastly, it was also advantageous that the model by Christensen *et al* (1982) is adaptable, meaning that, if the model was deemed to be too inaccurate, it is possible to convert the model to a more complex model without much alteration to the existing model, but rather by adding elements to the model. Because of all these reasons, it was decided to adapt the model by Christensen *et al* (1982) for use in the continuous Kraft digester.

3.4 Kraft model

The chosen batch Kraft model by Christensen *et al* (1982) is given below in Table 4. This is Equations 21 to 20 explained in Section 2.7.

Table 4: Christensen, Albright & Williams (1982) model equations.

Equation
$k_i = A_i \times \exp\left(\frac{-E_i}{RT_c}\right)$
$\frac{dL_1}{dt} = -[k_1(OH) + k_2(OH)^{0.5}(HS)^{0.5}] \times L_1$
$\frac{dL_2}{dt} = -[k_3(OH) + k_4(OH)^{0.5}(HS)^{0.5}] \times L_2$
$\frac{dC_1}{dt} = -[k_5(OH) + k_6(OH)^{0.5}(HS)^{0.5}] \times (C_1 - C_{1U})$
$\frac{dC_2}{dt} = -[k_7(OH) + k_8(OH)^{0.5}(HS)^{0.5}] \times (C_2 - C_{2U})$
$\frac{dC_3}{dt} = -[k_9(OH) + k_{10}(OH)^{0.5}(HS)^{0.5}] \times C_3$
$V_e = \frac{0.6m_{crit}}{\rho_{liq}(1-m_{crit})}$
$v_f = \frac{ltw_{ratio}}{\rho_{liq}}$
$\frac{d(OH)}{dt} = \frac{1}{V_e} [KA((OH)_f - (OH)) + (b_{COHL} - 0.5 \times b_{CSHL}) \times \left(\frac{dL}{dt} + b_{COHC} \times \frac{dC}{dt}\right)]$
$\frac{d(HS)}{dt} = \frac{1}{V_e} [KA((HS)_f - (HS)) + 0.5 \times b_{CSHL}] \times \left(\frac{dL}{dt}\right)$
$\frac{dX}{dt} = \frac{1}{V_e} \times [KA(X_f - X) - \frac{dW}{dt}]$
$\frac{d(OH)_f}{dt} = -\frac{1}{V_f} \times KA \times [(OH)_f - (OH)]$
$\frac{d(HS)_f}{dt} = -\frac{1}{V_f} \times KA \times [(HS)_f - (HS)]$
$\frac{d(X_f)}{dt} = -\frac{1}{V_f} \times KA \times [X_f - X]$

The model parameters can be found in Christensen *et al* (1982) and SI values for the reaction kinetics parameters can be found in Wisnewski *et al* (1997). This dissertation will be working in SI units and, because of this, the parameters and equations will be converted to SI units. As previously stated, this is a batch model and, therefore, the model

focuses on reaction kinetics. To adapt this model to a continuous process will present its own challenges, as will be discussed in Section 4 below. Although the model will undergo considerable changes, this Kraft model will form the foundation and backbone of this model. The model is fairly simple and elegant, without losing the ability to accurately predict the kinetics of the digester system. One of the drawbacks of this model is that it does not allow for the computation of the compaction factor of the pulp throughout the cook (unlike the model of Bhartiya *et al* (2003) for example). It was decided however, that this does not matter a great deal at the current phase of model implementation at Ngodwana and it was agreed that it will be possible to add it in the future with relative ease. Thus, this model was chosen for adaption. A similar approach was also followed by Rahman, Avelin & Kyprianidis (2019) during the modelling of a similar continuous digester.

4 Continuous model

The batch Kraft model by Christensen *et al* (1982) will be adapted for use on the continuous digester at Ngodwana. This will be done by looking at a systematic approach to the development of dynamic models given by Seborg *et al* (2011) and mentioned in Section 2.4.1. Firstly, the modelling needs of the continuous digester will be determined and then the model will be expanded to bridge the gap between this and the batch process model. The section title will correspond to the layout given in Section 2.4.1 above.

4.1 Continuous digester modelling needs

From Section 2.4.1, the first step is to decide upon the modelling objectives and end use of the model. Also, to decide upon the required levels of model detail and accuracy required. To adequately model the digester at Ngodwana, a model will need to satisfy some requirements and these will also form the modelling objectives. These include:

- Adequately model the internal dynamics of the digester. That is, capturing the continuous nature of the digester.
- Only rely on available and measurable inputs.
- Sufficiently account for reaction kinetics in the system.
- Yield outputs that are measurable and useful (most of all, accurate Kappa values)
- Incorporate the effects of an energy balance.
- Predict well over a reasonable range of process operation.

These needs should be met by the adapted model in order to decently simulate the continuous Kraft digester. When deciding upon the necessary levels of model accuracy and detail, these will greatly only be as accurate as the batch model that is worked from. From what can be told, the model by Christensen *et al* (1982) is accurate enough while still being fairly simple, without overwhelmingly complex detail.

4.2 Process schematic diagram

The second step is to draw the process schematic diagram and label all variables in the process. The process schematic diagram of the digester as received from Sappi can be seen in Figure 2 below:

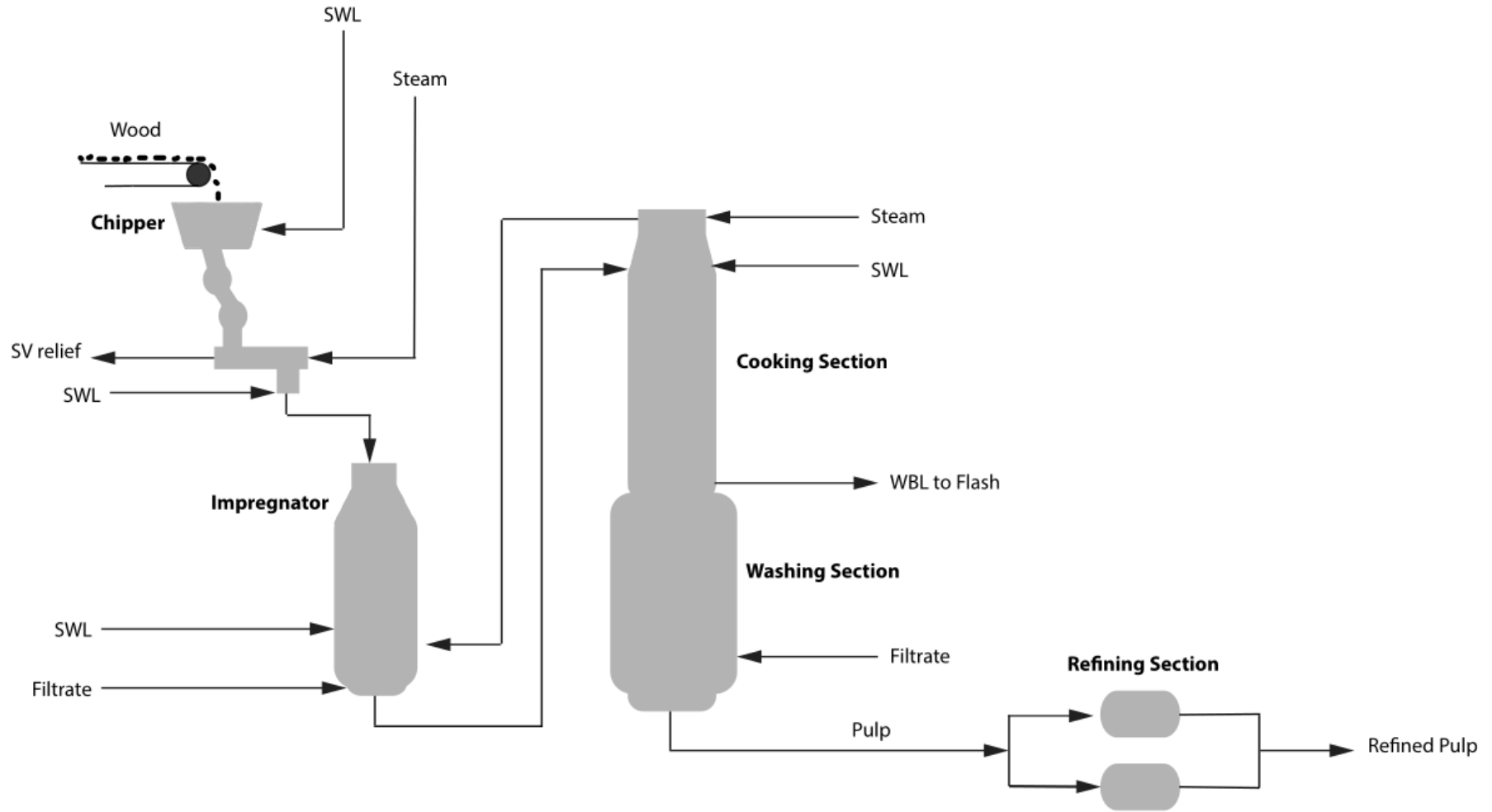


Figure 2: Schematic of the digester layout.

As Figure 2 illustrates, the wood enters the system and moves to the chipper. From there, the wood chips are mixed with strong white liquor (SWL) and heated with steam. It then enters the impregnation vessel. Here the wood is impregnated with liquor but, there is little reaction occurring since the temperature of the vessel is relatively low. Hereafter the impregnated chips and liquor move to the digester cook section. Here the bulk of the reaction takes place as this section is heated with steam. The next phase is then the washing section where the pulp is rinsed from the liquor and the spent liquor (weak black liquor or WBL) is removed. The pulp then passes on to refiners and after the refiners their lignin content is measured before it moves on to be processed further. This model will focus on the cooking section of the digester. To model the system without looking into the impregnation or washing section comes with some assumptions that will be discussed in Section 4.3 below. Figure 3 below shows the cooking section of the digester.

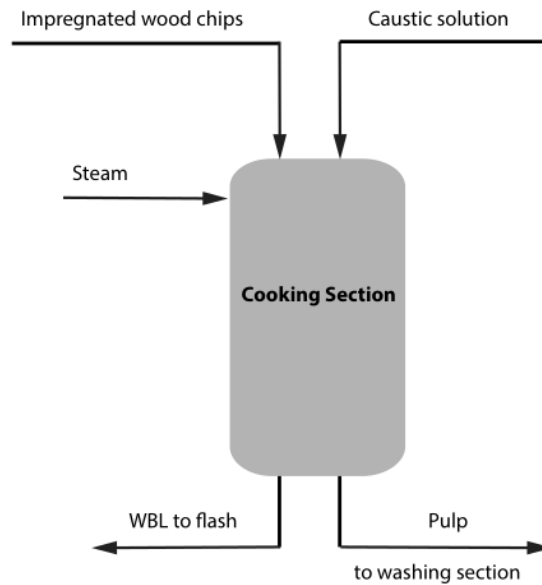


Figure 3: Schematic of the cooking section.

The variables of the systems will be examined next.

4.2.1 Model inputs

The inputs to the cooking section in Figure 3 above are shown in Table 5:

Table 5: Model inputs.

Input	Symbol	Unit	Description
Chip meter speed	S_{wood}	$\frac{rev}{min}$	Digester chip feed rate
Digester temperature	T_{cin}	K	Digester liquid temperature at top
Effective alkali (EA)	EA	$\frac{gNa_2O}{L}$	EA Concentration entering digester
Sulphidity	$Sulph$	$\frac{Na_2S}{Na_2S+NaOH} \%$	Sulphidity entering digester

Using the chip meter speed with the volume of the chip meter, a volumetric flow of chips can be determined. This, in combination with the liquor to wood ration, can be used to determine the volumetric flow rate of the caustic solution. The EA and sulphidity measurements give the caustic concentration and the temperature is also known from measurements.

4.2.2 Model outputs

The main outputs of the digester are given in Table 6 below:

Table 6: Model outputs.

Output	Symbol	Unit	Description
Kappa number of pulp	Kr		Measurement of end pulp lignin content
Temperature out	T_{out}	°C	Temperature of pulp leaving digester
Pulp composition out	m_{wi}	$\frac{kg_i}{kg_{pulp}}$	Mass fraction wood component in pulp
WBL composition out	m_{li}	$\frac{kg_i}{kg_{WBL}}$	Mass fraction caustic component in liquor

The most important output of the model is the Kappa number. The main goal of the digester is to break down the lignin from the wood pulp to a certain degree. Because of this, the Kappa number is of utmost importance as it is an indication of the lignin content. Furthermore, the ultimate goal of this project is to reduce the Kappa variance of the digester. Along with this, the Kappa number prediction is very important. The rest of the listed outputs are not of the utmost importance and many of them are not directly measured (therefore can not be compared to plant data). They can, however, still give insight into the state of the digester internals and are necessary in predicting the Kappa value. With this Step 1 and 2 as outlined in Section 2.4.1 are complete.

4.2.3 Kappa Measurements

From Section 4.2.2 above, it is clear that the Kappa prediction of the model is of the utmost importance. However, the model will predict the lignin content of the pulp leaving the digester and does not account for changes in the lignin content brought about by the refining section. The challenge in this is that the Kappa measurements on site can only be done on the pulp after it has passed through the refining section. Figure 4 below shows the locations of the three on site Kappa measurement locations.

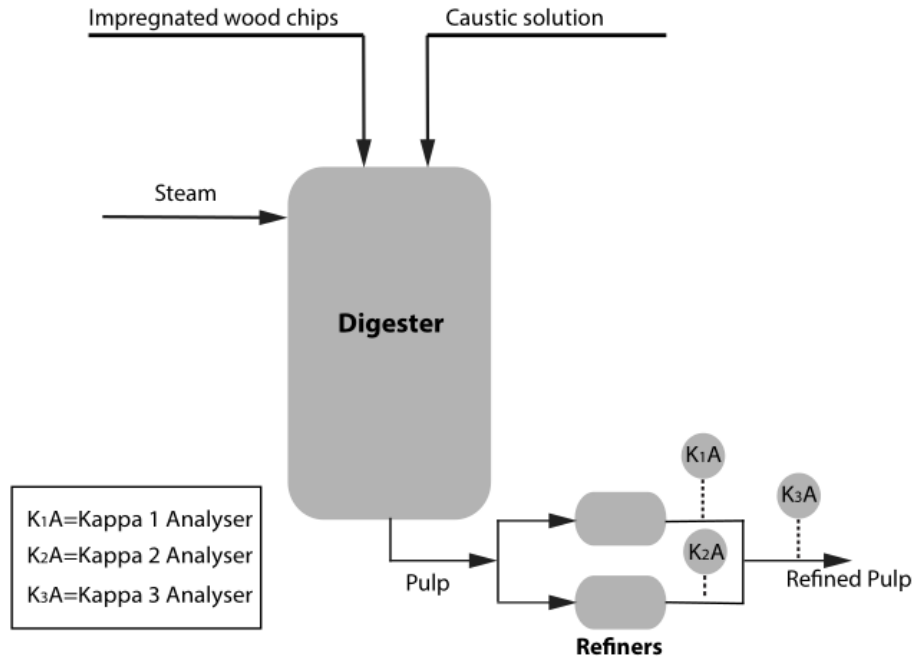


Figure 4: Kappa analyser 1, 2 and 3 location in relation to the digester.

4.3 Modelling assumptions

The implications of this will be discussed in greater detail in Section 7.2.1 below, however it is important to note that the measured and predicted values are expected to differ to some incalculable degree.

As mentioned in Section 2.4.1, any model of a physical system needs to rely on some modelling assumptions. This is also part of step 3 of modelling as outlined in Section 2.4.1. These might not hold perfectly true in all cases but it is assumed that, either the system will only very infrequently violate these assumptions, or if the system would violate the assumption, it will be small such that its effect is negligible. Some assumptions are better than others, but all assumptions aid in simplifying a system for easier modelling.

The modelling assumptions for this model are as follows and are very similar to the assumptions made by Christensen *et al* (1982) which is in turn similar to those made by Smith & Williams (1974).

1. The basic kinetic equations and correlations of the laboratory (or batch) units will hold for the continuous digester unit. This assumption is sensible, since the operation temperatures, reagent concentrations, sulphides and liquor to wood ratio are all similar (Christensen *et al*, 1982).
2. No back flow (also known as ideal plug flow) occurs for the wood chips in the digester. Although back flow does occur in industrial units, Christensen *et al* (1982) shows that there exists very little back flow in a typical digester. They also show

that the chips in a real process move at a rate through the reactor that is similar to what is predicted with this assumption. Therefore, the assumption is reasonable.

3. Compaction of chips in the digester is negligible. Although there would definitely be some effects from compaction, it is not included in the model for the sake of simplicity. It might be added in the future if it is deemed necessary. The effect of the compaction of the chips should not be great enough to drastically alter the results.
4. No back flow (also known as ideal plug flow) of the caustic solution occur in the continuous digester. This assumption seems sensible and has also been made by other investigators (Christensen *et al*, 1982; Bhartiya *et al*, 2003; Rahman *et al*, 2019). The assumption rests on the fact that continuous digester is totally filled with liquor and wood chips. The liquor then fills the space between the wood chips and move at a very low velocity down the digester. Uniform flow of liquor seems likely because the chips follow plug flow closely. Some exceptions to this assumption exists. These are:
 - (a) Liquor near the digester wall may not follow a precise plug flow pattern. This liquor, however, accounts for a small percentage of the total liquor volume, especially since the digester has a large diameter and therefore a high volume to surface ratio.
 - (b) Around the heating streams, there is some incoming or outgoing flow that will interfere with the liquid pattern. Here in the digester, the flow of liquor has both vertical and radial components, however this still only accounts for a small part of the digester.
 - (c) At the bottom of the digester, near the wash zone, up-flowing liquor meets down-flowing liquor from the cooking zone. This will lead to complicated flow patterns that are not accurately modelled, however, once again, this accounts for a small percentage of the liquor in the digester.
 - (d) Near liquor inlets and outlets in the top and bottom of the digester, plug flow seems unrealistic, however this is also a small part of the volume in question.

Thus, no backflow of liquor looks to be a sensible assumption, and can be modelled rather easily mathematically.

5. The temperature, caustic solution and wood component concentration remains constant throughout the radial direction of the digester. This assumption has also been made by numerous other investigations (Christensen *et al*, 1982; Bhartiya *et al*, 2003; Rahman *et al*, 2019). As with the previous assumption, there will be exceptions around the areas mentioned above.

- (a) Even though digesters are typically well insulated, the wall temperature will still likely be lower because of heat loss to the environment. This, along with wall retention of liquid and wood alike would likely yield differing concentrations at the digester wall.
- (b) Around the heating streams, there is some incoming or outgoing flow that will likely interfere with the flow patterns of both the liquid and the wood chips, causing radial variance. The temperature will also be affected, further interfering with the reaction and concentrations.
- (c) At the bottom of the digester, near the wash zone, the up-flowing liquor meets down-flowing liquor from the cooking zone. This leads to complicated flow patterns. This will also inevitably cause radial variance in both the caustic and wood compositions as well as in the temperature.

The assumption should be reasonable for between 80 and 90 % of the digester (Christensen *et al*, 1982). This assumption greatly reduces the mathematical intensity of the model.

- 6. Given the previous assumptions, the digester can be modelled as a plug flow reactor (PFR). Since a PFR would be complex to model (yielding partial differential equations for both volume and time), the PFR will be approximated as multiple smaller continuously stirred tank reactors (CSTRs) in series, each with the same cross-sectional area as the digester. This method will allow for prediction of conversion and composition throughout the digester.
- 7. Wood composition can be adequately modelled by only looking at lignin, cellulose, galactoglucomannan and araboxytan. This is sensible since most of the wood consists of these 5 components and the rest of the wood is also hemicelluloses which might react similarly to either galactoglucomannan or araboxytan.
- 8. Liquor to wood ratio remains constant. This should be reasonable since the digester controls the liquor to wood ratio to a specific value. If the moisture content of the wood should vary and the chemical dosing remains constant, this could vary significantly, however this is a simplifying assumption that needs to be made.
- 9. No reaction takes place in the impregnation vessel. This is a reasonable assumption since the relatively low temperature and retention time of the impregnation vessel do not allow for fast reactions.
- 10. No reaction takes place in the washing section of the digester. This is a fair assumption since the washing liquid has weak caustic concentration and the temperature is also reduced. There is a risk of back-precipitation of lignin here if the pH drops.

There needs to be enough alkali and temperature left to avoid this, however this is a simplifying assumption that needs to be made.

11. The Kappa number of the pulp is not influenced by the refiners. This is very likely a poor assumption. Kappa measurements by using UV absorption as with the online Kappa measurement devices may be affected significantly. This is nevertheless a necessary assumption since there is not enough data available to model the refiners or their effects as part of the digester. The Kappa measurements are not taken after the pulp leaves the digester, but rather after the refiners and therefore the measurements to which the model will be compared will have been altered by the refiners. This is discussed in greater detail in Section 7.2.1.

4.4 Spatial variations

The next step (step 4 outlined in Section 2.4.1) is to determine if spatial variations are of concern to the model. If it is the case, a partial differential equation will be necessary. From assumption 5 and, to a lesser extent, 6 above, it is clear that it is assumed that there exists no radial differences in the sections. Changes through the length of the digester are assumed and this will be addressed in Section 4.6 below.

4.5 Model composition

This Section, together with Section 4.6 below will serve as step 5 and 6 outlined in Section 2.4.1. Since numerous conservation equations as well as equilibrium relations and other algebraic equations from thermodynamics, chemical kinetics, equipment geometry and transport phenomena are included from the batch model, it was decided to take these two steps together with the adaptation to a continuous system. As mentioned in Section 4.3 under assumption 6 the model will simulate the digester by approximating it as multiple CSTRs in series. The model will therefore assume that the input for each digester section is the output of the section before it and that its starting state will be the same as its end state at the previous time step. This is clearly illustrated in Figure 5 below:

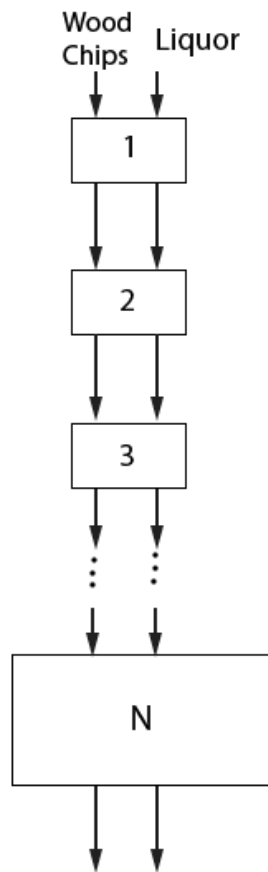


Figure 5: Illustration of CSTR approximation of digester.

The first step is to adapt the model by Christensen *et al* (1982) such that it can be applied to a single CSTR with given inputs. Hereafter, the model can be adapted to be applied to all the sections in series to yield the desired result.

CSTR model

The batch model by Christensen *et al* (1982) does not need a great deal of adaption to be applied to a CSTR. The larger challenge lies in converting the input variables into the variables used by the model.

4.5.1 Variables used

The model described below relies on numerous variables and parameters. These variables and parameters will be described below and parameter values will be displayed.

Parameters

The parameters used by the model are displayed in Table 7 below:

Table 7: Model parameters.

Symbol	Description	Value	unit
$V_{chipper}$	Volume of the chip feeder	0.697	$\frac{m^3}{rev}$
dt	Sampling time	0.1	min
MM_{NaOH}	Molar mass NaOH	40	$\frac{kg_{NaOH}}{kmol_{NaOH}}$
MM_{Na_2O}	Molar mass Na ₂ O	62	$\frac{kg_{Na_2O}}{kmol_{NaOH}}$
LTW	Liquor to wood ratio	3.7	$\frac{kg_l}{kg_w}$
ρ_L	Liquid density	1000	$\frac{kg_l}{m_L^3}$
ρ_C	Wood density	160	$\frac{kg_W}{m_W^3}$
A_{ji}	Pre-exponential constant	In Table 8	$\frac{m^3}{kgmin}$
E_{ji}	Activation energy	In Table 8	$\frac{kJ}{kmolK}$
R	Universal gas constant	8.314	$\frac{kJ}{kmolK}$
V	Volume of assumed CSTR	10	m^3
m_{crit}	Critical moisture content	0.65	$\frac{kg_L}{kg_{ODW}}$
b_{cohl}	Consumption constant	0.166	$\frac{kg_{NaOH}}{kg_{Lignin}}$
b_{cshl}	Consumption constant	0.395	$\frac{kg_{NaOH}}{kg_{Lignin}}$
b_{coch}	Consumption constant	0.039	$\frac{kg_{NaOH}}{kg_{Cellulose}}$

Table 7 references pre exponential constants as well as activation energies. These were obtained from Wisniewski *et al* (1997) since they present it in SI units whereas the paper by Christensen *et al* (1982) gives it in Imperial units. These values are given in Table 8 below:

Table 8: Kinetic Reaction Parameters by Wisniewski, Doyle & Kayihan (1997).

	1	2	3	4	5
A_{1i}	2.8×10^{-1}	6.04×10^{10}	6.45	1.56	1.02×10^4
A_{2i}	9.26	4.9×10^{-1}	2.809×10^1	1.041×10^1	5.72×10^{16}
E_{1i}	2.93×10^4	1.15×10^5	3.47×10^4	2.51×10^4	7.32×10^4
E_{2i}	3.14×10^4	3.77×10^4	4.18×10^4	3.77×10^4	1.67×10^5

Various intermediate variables are also determined to aid in calculation. These are given in Table 9 below:

Table 9: Intermediate variables.

Symbol	Description
F_w	Volumetric wood flow rate
F_{SWL}	Volumetric SWL flow rate
NaOH	Concentration of OH in unused units
Na ₂ S	Concentration of HS in unused units
$C_{OH_{in}}$	Concentration of OH in correct units
$C_{SH_{in}}$	Concentration of HS in correct units
$m_{i_{in}}$	Wood component mass flow into assumed CSTR
$m_{i_{out}}$	Wood component mass flow out of assumed CSTR
k_{ji}	Reaction rate constant
Rs_i	Rate of reaction of wood component i
$\frac{dL}{dt}$	Mass change of lignin in the assumed CSTR
$\frac{dC}{dt}$	Mass change of cellulose in the assumed CSTR
$m_{w_{in}}$	Total wood mass flow into assumed CSTR
$m_{l_{in}}$	Total liquid mass flow into assumed CSTR
V_e	Volume of entrapped liquid
V_f	Volume of free liquor
r_{OH}	Rate of reaction of OH in entrapped liquid
r_{SH}	Rate of reaction of HS in entrapped liquid
r_{OH_f}	Rate of reaction of OH in free liquid
r_{SH_f}	Rate of reaction of HS in free liquid
E_{gen}	Energy generated by reactions in assumed CSTR
$KAdV$	mass transfer coefficient times mass transfer area per entrapped volume
KA	mass transfer coefficient times mass transfer area

Table 10 contains various variables that are treated as parameters, however they are not fixed parameters and might change from simulation to simulation however they are kept constant throughout the simulation.

Table 10: Input parameters.

Symbol	Description	Value
x_{in}	Mass fraction of component i in wood	[0.15, 0.11, 0.43, 0.15, 0.17]
C_{OH}	Initial entrapped OH Concentration in CSTR	0
C_{SH}	Initial entrapped HS Concentration in CSTR	0
m_i	Mass of component i in CSTR initially	$1700x_{in}$
m_w	Total mass of wood in CSTR initially	1700
x_{∞}	Mass fraction non-reactive wood component	[0, 0, 0.25, 0.71, 0]
C_{OH_f}	Concentration in free liquid in CSTR initially	0
C_{SH_f}	Concentration in free liquid in CSTR initially	0
T_c	Temperature in CSTR initially	First measurement of T_{cin}

The output variables are then lastly given in Table 11 below:

Table 11: Model outputs.

Symbol	Description
$\frac{dM_i}{dt}$	Change in mass of wood component i in assumed CSTR
$\frac{dC_{OH}}{dt}$	Change in entrapped OH concentration in assumed CSTR
$\frac{dC_{SH}}{dt}$	Change in entrapped HS concentration in assumed CSTR
$\frac{dC_{OH_f}}{dt}$	Change in free OH concentration in assumed CSTR
$\frac{dC_{SH_f}}{dt}$	Change in free OH concentration in assumed CSTR
$\frac{dT_c}{dt}$	Change in Temperature in assumed CSTR
$Kappa_{CSTR}$	Kappa number inside CSTR

4.5.2 Inputs

Firstly the inputs will be converted such that it can be used in the model. A detailed account of variables used are visible in Tables 7 to 11 below. The conversion of the chip meter speed to volumetric flow rate of wood is given in Equation 39 below:

$$F_w = S_{wood}V_{chipper} \quad (39)$$

From here, the volumetric flow rate of liquor can also be determined using Equation 40 below:

$$F_l = \frac{LTW}{\rho_L} \rho_C F_w \quad (40)$$

The incoming mass of wood components are determined using Equation 41 below:

$$m_{i_{in}} = \rho_C F_w x_{in} \quad (41)$$

and the mass of wood components leaving the CSTR is given by Equation 42 below:

$$m_{i_{out}} = \frac{m_i}{V} F_w \quad (42)$$

Temperature is in units of °C and needs to be converted to K. This is done in Equation 43 below:

$$T_{cinK} = T_{cin} + 273 \quad (43)$$

The more difficult conversions are for the caustic solution concentrations. The effective alkali (EA) needs to be converted to concentration of hydroxide. Although both have similar units, namely $\frac{g_{Na_2O}}{L}$ (or $\frac{kg_{Na_2O}}{m^3}$) vs $\frac{kg_{NaOH}}{m^3}$, they are not equivalent. EA is defined by Equation 44 below:

$$EA = NaOH + Na_2S \quad (44)$$

Furthermore, the sulphidity needs to be converted to concentration of hydrosulphide. Sulphidity (S_r) is defined by Equation 45 below:

$$S_r = \frac{Na_2S}{Na_2S + NaOH} \quad (45)$$

Firstly, the EA from the input (or EA_{in}) needs to be converted from $\frac{kg_{Na_2O}}{m^3}$ to $\frac{kg_{Na_2O}}{kg_{ODW}}$. This is done by Equation 47 below:

$$v_f = \frac{LTW}{\rho_l} \quad (46)$$

$$EA_c = EA_{in} \times v_f \quad (47)$$

From here, the NaOH and Na₂S concentrations can be determined. Equations 48 and 49 follow from Equations 44 and 45 above.

$$Na_2S_c = EA_c \times S_r \quad (48)$$

$$NaOH_c = EA_c - Na_2S_c \quad (49)$$

Both NaOH_c and Na₂S_c have units of $\frac{kg_{Na_2O}}{kg_{ODW}}$ and need to be converted to have units of $\frac{kg_{NaOH}}{m^3}$. This is done in Equations 50 and 51 below:

$$NaOH = \frac{1}{v_f} NaOH_c \times \frac{2MM_{NaOH}}{MM_{Na_2O}} \quad (50)$$

$$NaSH = \frac{1}{v_f} \left(\frac{1}{2} Na_2S_c \right) \times \frac{2MM_{NaOH}}{MM_{Na_2O}} \quad (51)$$

The inputs are now converted such that they can be used in the model by Christensen *et al* (1982). NaOH and NaSH are the concentrations of the incoming stream to the

CSTR thus $\text{NaOH} = C_{OH_{in}}$ and $\text{NaSH} = C_{SH_{in}}$.

4.5.3 Reaction kinetics

The reaction kinetics are obtained directly from Christensen *et al* (1982) and no adjustments were made. The rate of reaction of wood components are given by Equations 52 and 53 below:

$$k_{ji} = A_{ji} \exp \frac{-E_{ji}}{RT_c} \quad (52)$$

$$Rs_i = -(k_{1i}C_{OH_e} + k_{2i}(C_{OH_e})^{0.5}(C_{SH_e})^{0.5})\left(\frac{m_i}{m_w} - x_\infty\right)m_w dt \quad (53)$$

where i refers to any one of the 5 wood components and the subscript e refers to the concentration entrapped in the wood. This gives the change in mass of all wood components given a certain time difference. Along with the wood components, the caustic solution also changes. The caustics consist of 2 areas namely the free and entrapped liquor where the free liquor refers to the liquor that moves freely between the wood chips and pulp and the entrapped liquor refers to the liquid that has been absorbed by the wood and is entrapped in the woody matrix. It is this entrapped liquor that is referred to with the subscript e . The change in caustic solution is reliant on some intermittent variables such as the KA term, volume of entrapped liquor and the likes. These equations will be discussed below: The entrapped liquid fills a certain volume inside the wood based on how much liquid the wood can absorb. This entrapped volume (v_e) is given in units of $\frac{\text{m}^3}{\text{kg}_{ODW}}$ and is determined by Equation 54:

$$V_e = \frac{0.6m_{crit}}{\rho_L(1 - m_{crit})} \quad (54)$$

The KA gives an indication of mass transfer between free and entrapped liquor. It is a function of temperature of the wood and is calculated using Equation 55 below:

$$KAdV = \begin{cases} 3.8 \times 10^{-5}(T_c - 273) - 1.1 \times 10^{-3} & T_c \leq 373\text{K} \\ 6.6 \times 10^{-5}(T_c - 273) - 3.9 \times 10^{-3} & 373\text{K} \leq T_c \leq 423\text{K} \\ 1.2 \times 10^{-4}(T_c - 273) - 1.2 \times 10^{-2} & 423\text{K} \leq T_c \end{cases} \quad (55)$$

To convert $KAdV$ to the correct units, Equation 56 is employed.

$$KA = 60KAdV \times dt \times V_e \quad (56)$$

Another useful intermediate variable is simply the sum of the mass of all the wood components in the CSTR, effectively giving the mass of wood in the CSTR. This is

illustrated by Equation 57 below:

$$m_w = \sum_i m_i \quad (57)$$

with m_i denoting the mass of wood component i in the CSTR.

Another important variable is $\frac{dL}{dt}$ and $\frac{dC}{dt}$ given by Equations 58 and 59 below. They denote the change in lignin (sum of change in slow and fast reacting lignin) and the change in carbohydrates (sum of change in cellulose and hemicelluloses)

$$\frac{dL}{dt} = R_{s1} + R_{s2} \quad (58)$$

$$\frac{dC}{dt} = R_{s3} + R_{s4} + R_{s5} \quad (59)$$

Finally, with all these variables defined, the reaction kinetics of the caustics can be discussed. The exchange between the free liquor and the entrapped liquor and then again between the entrapped liquor and the wood components are described by Equation 60 to 63 below:

$$r_{OH} = \frac{1}{V_e} (KA(C_{OH_f} - C_{OH_e}) + (b_{cohl} - 0.5b_{cshl})\frac{dL}{m_w dt} + b_{coch}\frac{dC}{m_w dt}) \quad (60)$$

$$r_{SH} = \frac{1}{V_e} (KA(C_{SH_f} - C_{SH_e}) + 0.5b_{cshl}\frac{dL}{m_w dt}) \quad (61)$$

$$r_{OH_f} = \frac{-1}{V_f} KA(C_{OH_f} - C_{OH_e}) \quad (62)$$

$$r_{SH_f} = \frac{-1}{V_f} KA(C_{SH_f} - C_{SH_e}) \quad (63)$$

It should be noted again that these reaction kinetics were developed by empirically fitting equations to measurements that were made. They all predict the reactions well, although they are not first principal models with chemistry in mind. The reaction kinetics predict the main wood components well but the model does not predict the rate of reaction of all the byproducts that form. the model does not have equations for the byproducts and will therefore not be able to track their concentrations. If they are deemed important enough, they can be added to the model, although some experimentation might be needed to determine these lesser reaction kinetics.

The only remaining part of the CSTR model is the flow dynamics which will be discussed below:

4.5.4 Reactor dynamics

Mass balance

The main mass balance equation is given below as Equation 64:

$$\frac{dm}{dt} = m_{in} - m_{out} + m_{generated} \quad (64)$$

This equation can be adapted to be used to calculate the wood component mass balance as well as the caustic solution mass balance. The wood component mass balance is given in Equation 65 below:

$$\frac{dm_i}{dt} = m_{i_{in}} - m_{i_{out}} + m_{i_{generated}} \quad (65)$$

with $m_{i_{generated}} = Rs_i$.

Similarly, the mass balance for the caustic solution can be determined. This is done in Equation 66 below, however, the mass balance is set up to accept a change in concentration for generated mass:

$$\frac{dC_i}{dt} = \frac{m_{i_{in}} - m_{i_{out}} + m_{i_{generated}}}{v_k \times m_w} \quad (66)$$

with i denoting OH, OH_f, SH or SH_f and v_k denoting v_e for entrapped concentrations and v_f for free concentrations. Equation 66 can be rewritten to Equation 67 below:

$$\frac{dC_i}{dt} = \frac{F_l(C_{i_{in}} - C_{i_{out}})}{v_k \times m_w} + r_i \quad (67)$$

with F_l being the volumetric flow rate of liquor into and out of the CSTR from Equation 40.

The energy balance needs to be described. Equation 68 below yields the change in temperature over time:

$$\frac{dT_c}{dt} = \frac{(m_{w_{in}}cp_w + m_{l_{in}}cp_l)(T_{c_{in}} - T_{c_{out}}) - hA(T_c - T_{ambient}) + \sum \frac{dm_i}{dt} \lambda}{(m_w cp_w + m_l cp_l)} \quad (68)$$

However, herein lies a problem. Not only is the cp of the pulp unknown (both cp_w and cp_l), there is also no information on the heat loss due to convection on the outside of the digester. Along with this, neither lignin nor hemicelluloses have well-defined molar masses, so heat of reaction is difficult to determine. Because of this, the energy balance equation was built with cp_w , cp_l and h as adjustable parameters to ensure the best fit for optimizers etc. This is all the necessary information to model a CSTR using the model by Christensen *et al* (1982).

The last part is to ensure the output is returned sensibly. Since the residual lignin content

is described by the Kappa number, this needs to be specified. The Kappa number is calculated using Equation 69 below:

$$Kappa_{CSTR} = \frac{100(m_1 + m_2)}{0.13m_w} \quad (69)$$

4.5.5 Simulation

The model equations mentioned above were transferred to a computer simulation coded in Python. This simulation consists of two parts. The first part (called the modelling section) consists of the model equations mentioned above, whereas the second part (called the simulating section) of the simulation is responsible for integrating the differential equations in the modelling section. The simulating sections utilizes Euler integration regarding time to accomplish this. This is done creating a loop, with each instance of the loop concerned with the following time step. Given initial conditions for the states of the model, the differential equations are then used to determine the changes that occur in the states of the model at this given instance. The states are then updated with these changes and the process is repeated. Giving an adequately small time step value ensures that the errors made by integrating over finitely large time steps (as opposed to infinity small time steps) are negligible. It is important that the time step be chosen small enough as mentioned, however, a too small time step could cause excessive increases in computing and, therefore, simulation time. A time step of 0.1 minutes (or 6 seconds) was chosen. The reason for this is that, with unknown initial conditions, high initial answers were often obtained from the differential equations (corresponding to a large and sudden change in the system). This is a result of the system's initial conditions not being at equilibrium with the inputs. This is expected and not a problem with small time steps, since the simulation soon reaches the aforementioned equilibrium, however, as the time steps increase, problems arise. The reason for this is that, at large time steps, the large differential is continued for a longer time. Thus, the longer the time steps, the greater the risk of destabilizing the system. With all this in mind, through trial and error, it was found that 0.1 minute yields an acceptable execution time and is short enough to ensure stability of the model. The pseudo-code below should illustrate the setup of the simulation.

Listing 1: Pseudo-code illustrating batch simulation setup

```

states = initial_states
delta_t = time_range[1] - time_range[0]
for t in time_range:
    inputs = obtain_inputs(t)
    derivatives = model_section(inputs, states)*delta_t
    states = states + derivatives
  
```

```
Kappa = Kappa_function(states)
save_Kappa(Kappa)
plot(time_range, Kappa)
```

To further illustrate the method used, take the first three time steps of the simulator. Firstly, the CSTR section uses the steady state input values as input and uses the model equations and its current state to determine its state after six seconds. After this calculation, the CSTR as before, uses the steady state input values as input and uses the model equations and its current state its state after a further 6 seconds. This then continues for 200 minutes worth of simulation time (2000 time steps). The libraries utilized from Python are listed in Table 12 below:

Table 12: Used Python libraries.

Library	Version
numpy	1.19.2
pandas	1.1.3
matplotlib	3.3.2

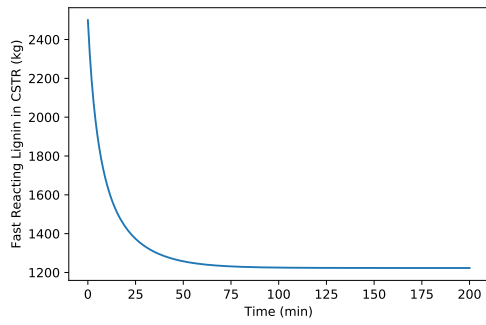
4.5.6 Results

After the CSTR equations are set up as detailed in Section 4.5.5 above, it was used to test the model to ensure it acts as expected. The following results were obtained (Figures 6 and 7 below). The input conditions were chosen fairly arbitrarily and are listed in Table 13 below. All variables not listed are assumed to have the values declared in Tables 7 to 11.

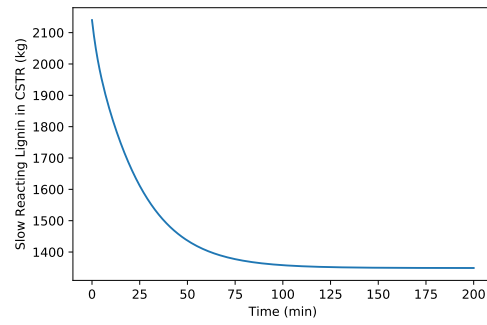
Table 13: Initial values to CSTR simulation.

Symbol	Description	Value	unit
Set parameters			
$Volume$	Volume of CSTR	1000	m^3
Δt	Time step used in Euler integration loop	1	min
LTW	Liquor to wood ratio	3.7	$\frac{kg_{SWL}}{kg_{ODW}}$
Initially states in CSTR			
OH_{e0}	Concentration entrapped OH in CSTR	70	$\frac{kg_{NaOH}}{m^3}$
SH_{e0}	Concentration entrapped SH in CSTR	50	$\frac{kg_{NaOH}}{m^3}$
OH_{f0}	Concentration free OH in CSTR	85	$\frac{kg_{NaOH}}{m^3}$
SH_{f0}	Concentration free SH in CSTR	50	$\frac{kg_{NaOH}}{m^3}$
Tc_0	Temperature of CSTR	418	K
m_{w1_0}	Weight of slow lignin in CSTR	2500	kg
m_{w2_0}	Weight of fast lignin in CSTR	2140	kg
m_{w3_0}	Weight of cellulose in CSTR	6230	kg
m_{w4_0}	Weight of araboxylan in CSTR	2500	kg
m_{w5_0}	Weight of galactoglucomannan in CSTR	2700	kg
Steady state Inputs			
EA_{in}	Effective Alkali to CSTR	88	$\frac{kg_{Na_2O}}{m^3}$
$sulphidity_{in}$	Sulphidity to CSTR	0.28	
Tc_{in}	Temperature to CSTR	418	K
$m_{w1_{in}}$	Weight of slow lignin to CSTR	85.8	kg
$m_{w2_{in}}$	Weight of fast lignin to CSTR	65.9	kg
$m_{w3_{in}}$	Weight of cellulose to CSTR	245.2	kg
$m_{w4_{in}}$	Weight of araboxylan to CSTR	84.1	kg
$m_{w5_{in}}$	Weight of galactoglucomannan to CSTR	98.2	kg
fw	Volumetric flow rate of wood to digester	3.5	m^3

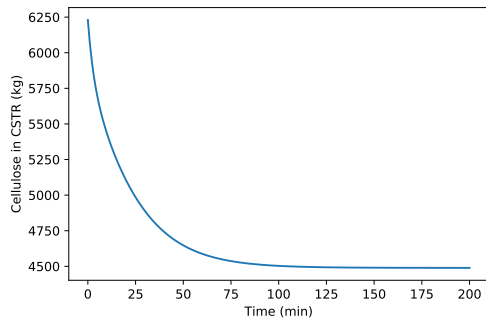
The simulation was run for 200 minutes of simulated time (2000 time steps) and these plots in Figures 6 and 7 below were obtained. The plots show the respective internal state variable of the CSTR. The reaction values here are of no value, since if different initial values were chosen, the results would change. The main goal of this illustration is to see if the model behaves as expected, meaning the curves are smooth and in a sensible direction. This is to test that the model setup was successful.



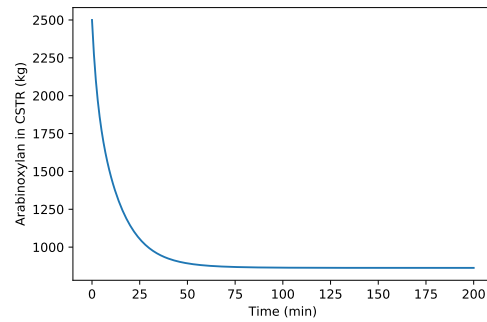
(a) Fast lignin content



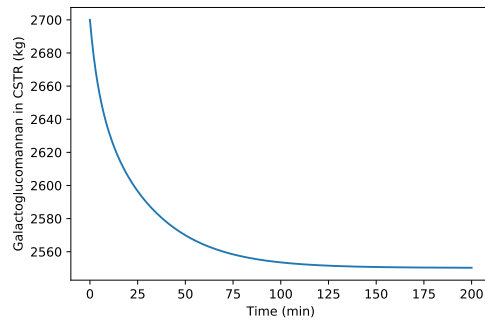
(b) Slow lignin content



(c) Cellulose content



(d) Araboxyylan content



(e) Galactoglucomannan content

Figure 6: Wood components in CSTR over time.

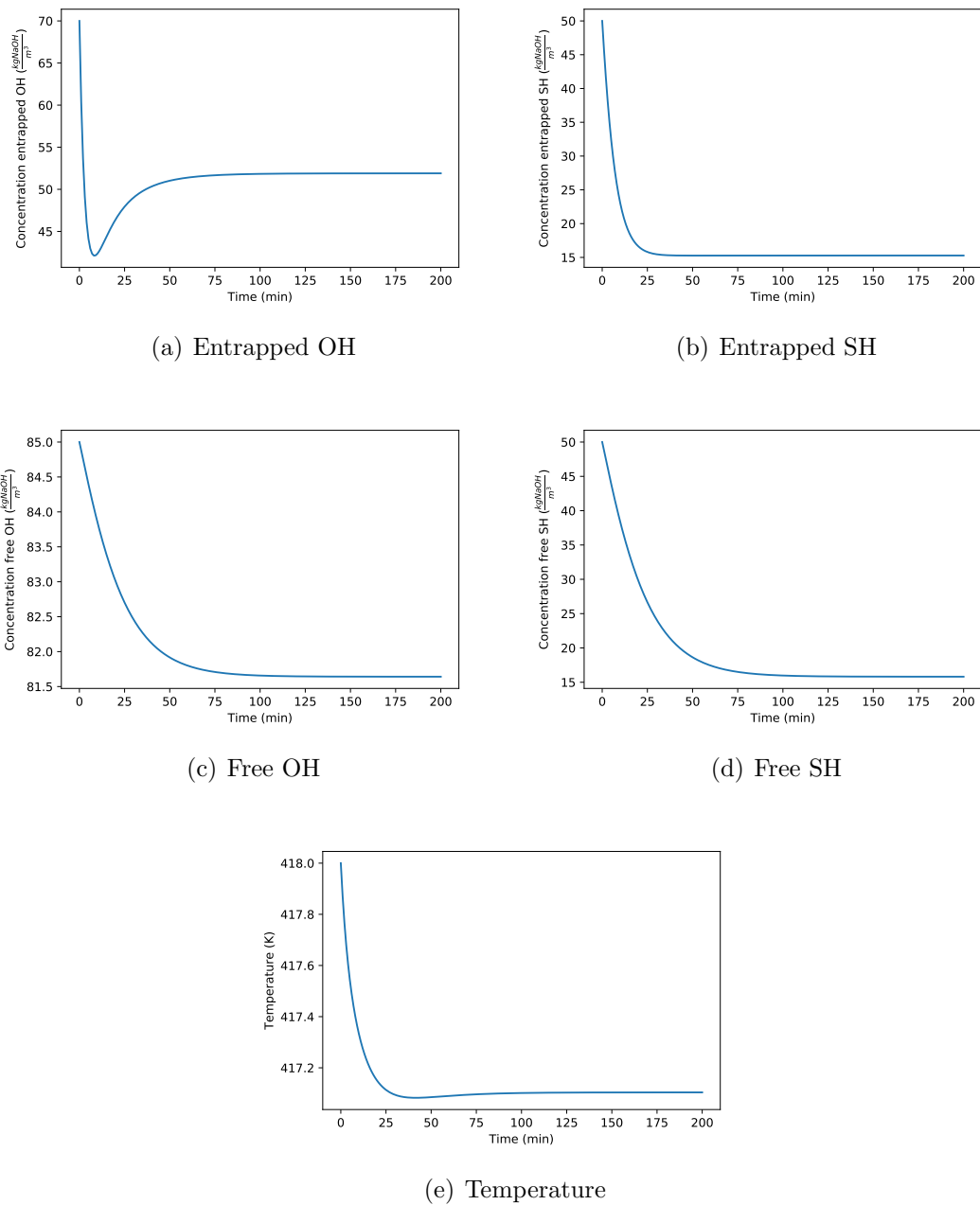


Figure 7: Caustic solution and temperature over time.

From the results of the CSTR, it is clear that the model is stable and able to predict the reactions to some extent. This is shown by the fact that the curves are all smooth and result proceed to steady state after some time. The reaction also progress as expected (for example the fast reacting lignin reacts faster than the slow reacting lignin). The CSTR model is sufficient to apply it to a larger simulation of various CSTRs in series as an approximation to the digester.

4.6 Model synthesis

This digester model proposed above contains states that change in two dimensions. The states change over time as well as throughout the volume of the digester. Therefore, the internal state of the digester (be it caustic concentration or temperature) will be different at different volumes of the digester as well as at different times. Because of the assumptions made in Section 4.3, the radial direction of the digester is an example of a dimension that will remain constant given a certain time and volume throughout the digester being modelled. This yields an interesting problem which, in turn, yields an interesting solution. The model can essentially be viewed as partial differential equations and the method of lines were chosen to ease the complexity of the solution. As mentioned in Section 2.8, the method of lines relies on choosing one dimension and discretizing all the others. In this case it was decided that time should be a simple dimension to keep continuous and to discretize the volume of the digester. This then approximates the digester to be a series of volumes for calculation purposes and time is then kept continuous. These volumes, in turn, are then assumed to act as CSTRs, as mentioned in Section 4.3 and on Figure 5.

This splits the variables in the model into two broad categories. These categories are then variables that move mainly with time and variables that changes mainly with volume. This is perhaps better explained by looking at the effects of these variables. The variables in the first category (which will be titled the state category), the variables that change mainly with time, will be the states of the individual CSTRs, whereas the second category (which will be titled the flow category) will be for variables that transport mass or energy to the following CSTR. The variable breakdown can be seen in Table 14 below:

Table 14: Distinction between state and flow variables in CSTR.

State category (in CSTR)		Flow category (Incoming)	
Variable	Description	Variable	Description
OH_{e0}	Entrapped OH concentration	OH_{ein}	Entrapped OH concentration
SH_{e0}	Entrapped SH concentration	SH_{ein}	Entrapped SH concentration
OH_{f0}	Free OH concentration	OH_{fin}	Free OH concentration
SH_{f0}	Free SH concentration	SH_{fin}	Free SH concentration
T_{c0}	Temperature	T_{cin}	Temperature
m_{w10}	Fast lignin mass	m_{w1in}	Fast lignin mass
m_{w20}	Slow lignin mass	m_{w2in}	Slow lignin mass
m_{w30}	Cellulose mass	m_{w3in}	Cellulose mass
m_{w40}	Araboxylan mass	m_{w4in}	Araboxylan mass
m_{w50}	Galactoglucomannan mass	m_{w5in}	Galactoglucomannan mass

At the first CSTR, the Flow variables will be calculated from the inputs to the digester, however, from there, the incoming variables need to be determined from the state variables from the previous digester at the end of the previous time step. This is then strung together to obtain the model for the continuous digester. This effect can be seen illustrated in Figure 8 below. Figure 8 is similar though more complete than Figure 5

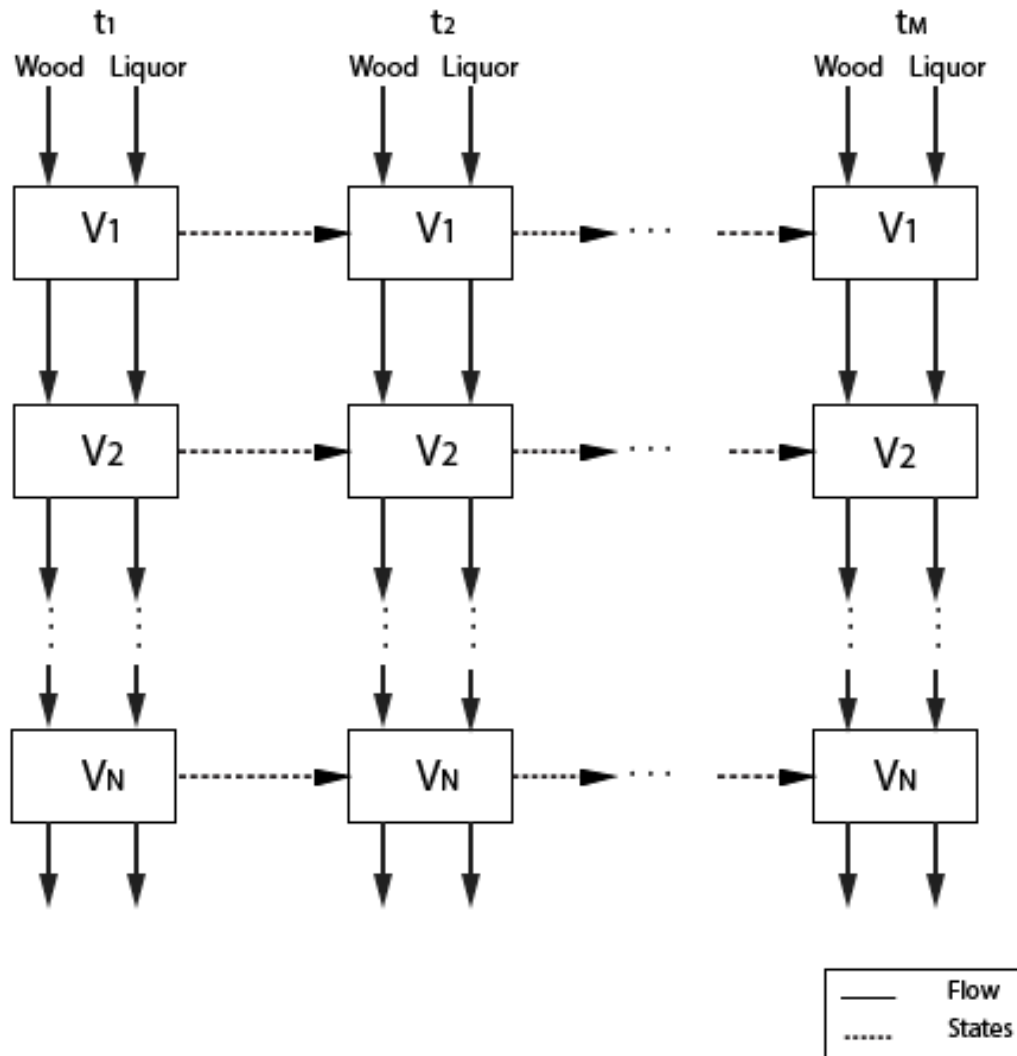


Figure 8: Illustration of the CSTR approximation with respect to volume and time.

4.7 Degrees of Freedom analysis

As step 7 outlined in Section 2.4.1, a DOF analysis needs to be done. Below is the equation for the Degrees of Freedom as given in Equation 2 in Section 2.4.1 above.

$$N_F = N_V - N_E$$

With N_V being the total number of process variables and N_E the number of independent model equations. The first step is then to determine the total number of variables. Looking at Table 7, there are 33 parameters (together with Table 8) and Table 9 reveals 49 intermediate variables. Do note that in both Tables mentioned, some variables are denoted with an i as subscript, resulting in 5 variables. Table 10 yields 17 input parameters and Table 11 yields 11 model outputs. Table 5 shows 4 model inputs. From Section 4.5.2, there are 13 model equations. Section 4.5.3 yields 20 model equations and Section 4.5.4 has 17 (do note that Equation 64 is not counted as it was merely used to derive Equation 65). Taking Equation 2 as mentioned before, the resulting DOF yields:

$$N_F = (33 + 49 + 17 + 11 + 4) - (13 + 20 + 17) = 114 - 60 = 54 \quad (70)$$

With 54 degrees of freedom, 54 variables are needed to fully specify the system. As alluded to earlier, these would be the parameter and input variables mentioned above. They account for 33 parameters, 17 input parameters and 4 inputs, fully specifying the system and bringing the DOF to 0.

4.8 Model simplification

During the composition of the model it became clear that the complexity of the model is adequate and it was decided that the model will not be simplified further. Another reason for this decision was that the intermediate variables currently available, do serve a purpose to the model. This then concludes step 8 as outlined in Section 2.4.1

4.9 Input distinction

The final step (step 9) in the process outlined in Section 2.4.1 is to distinguish between disturbances and manipulated input variables. The inputs from Table 10 and 5 is discussed below:

Initial conditions in the digester. These include entrapped and free concentrations of OH and HS, mass of wood and its components as well as the initial temperature. These variables are measurable and manipulable, however they are rarely manipulated and are rather described as parameters.

x_{in} Mass fraction of component i in wood in the feed. This is a disturbance variable since it is a function of the wood species and various other environmental factors that can not be manipulated. This denotes the total of component i in the wood feed. Not all of this will be able to react.

x_{∞} Mass fraction non-reactive wood component. This is not expected to change greatly but might be regarded as a disturbance. Some of component i will be unreactive

and will remain at the end of the digester. the reasons for this are discussed in Section 2.7.

Digester chip feed rate is a manipulable variable.

Digester liquid temperature at top of digester is a manipulable variable.

EA Concentration entering digester is a manipulable variable.

Sulphidity entering digester is a manipulable variable.

With the last step complete, this concludes the model.

4.10 Simulation Addition

The simulation mentioned in Section 4.5.5 was only for a batch digester. The model needed to be added upon to ensure an accurate prediction of a continuous system. This is accomplished by adding a loop to the already existing time loop, the second one being for volume. In keeping with the method of lines and division of the digester into numerous smaller CSTRs, the second loop will be nested inside the first. This ensures that, for every time step, a simulation, similar to that of Section 4.5.5, is run for every digester segment. The input to the first digester segment will be the inputs to the digester whereas every subsequent digester segment's input would be the output of the previous segment at the previous time step. The state of every section at the start of any given time step would be the final state of that segment from the previous time step. The flow rates into and out of the digester segments are dictated by the flow rate of wood and caustic solution into the digester. A segment volume of 10 m³ was chosen and was deemed small enough to give an accurate representation of the system. Given the nominal flow rates of the digester, it was found that each digester segment has a retention time of slightly less than a minute. With this knowledge, the time step of 0.1 minute was maintained and gave adequate results. The pseudo-code below should illustrate the setup of the simulation.

Listing 2: Pseudo-code illustrating continuous simulation setup

```
delta_t = time_range[1] - time_range[0]
for ti, t in enumerate(time_range):
    for vi, v in enumerate(volume_range):
        if vi == 0:
            inputs = obtain_inputs(t)
        else:
            inputs = result[ti, vi-1]
    if ti == 0:
        states = initial_states
```

```
else:  
    states = result [ti-1, vi]  
    derivatives = model_section(inputs, states)*delta_t  
    states = states + derivatives  
    result [ti, vi, :] = states  
    Kappa = Kappa_function(states)  
    save_Kappa(Kappa)  
plot(time_range, Kappa)
```

5 Results

After the simulation was constructed as outlined in Section 4.5.5 and expanded upon as described in Section 4.10, it was possible to use the simulation to put the model to the test. With this it will be possible to determine the accuracy of the model, as well as its advantages and shortcomings.

5.1 Preliminary model testing

The model as described in Section 4 was built using the Python programming language and was used to simulate the digester. The initial test, just to ensure that it operates as expected, was done with constant inputs to ensure the model is stable. These initial values are given in Table 15 below. Initially the states of the digester might not be known and, because of this, the initial states are assumed to be chosen probable values (comparable to values used in Table 13 above with the CSTR simulation).

Table 15: Initial values to steady input digester simulation.

Symbol	Description	Value	unit
Set parameters			
$Volume$	Volume of CSTR sections	10	m^3
Δt	Time step used in Euler integration loop	0.1	min
LTW	Liquor to wood ratio	3.7	$\frac{kg_{SWL}}{kg_{ODW}}$
Initially states in all CSTRs			
OH_{e0}	Concentration entrapped OH in CSTR	70	$\frac{kg_{NaOH}}{m^3}$
SH_{e0}	Concentration entrapped SH in CSTR	50	$\frac{kg_{NaOH}}{m^3}$
OH_{f0}	Concentration free OH in CSTR	85	$\frac{kg_{NaOH}}{m^3}$
SH_{f0}	Concentration free SH in CSTR	50	$\frac{kg_{NaOH}}{m^3}$
Tc_0	Temperature of CSTR	418	K
m_{w1_0}	Weight of slow lignin in CSTR	250	kg
m_{w2_0}	Weight of fast lignin in CSTR	214	kg
m_{w3_0}	Weight of cellulose in CSTR	623	kg
m_{w4_0}	Weight of araboxylan in CSTR	250	kg
m_{w5_0}	Weight of galactoglucomannan in CSTR	270	kg
Steady state Inputs			
EA_{in}	Effective Alkali to 1st CSTR	88	$\frac{kg_{Na_2O}}{m^3}$
$sulphidity_{in}$	Sulphidity to 1st CSTR	0.28	
Tc_{in}	Temperature to 1st CSTR	418	K
$m_{w1_{in}}$	Weight of slow lignin to 1st CSTR	85.8	kg
$m_{w2_{in}}$	Weight of fast lignin to 1st CSTR	65.9	kg
$m_{w3_{in}}$	Weight of cellulose to 1st CSTR	245.2	kg
$m_{w4_{in}}$	Weight of araboxylan to 1st CSTR	84.1	kg
$m_{w5_{in}}$	Weight of galactoglucomannan to 1st CSTR	98.2	kg
fw	Volumetric flow rate of wood to digester	3.5	m^3

The results that followed from the test can be seen in Figures 9 to 10 below. The plots show the various concentration and temperature profiles throughout the digester from top to bottom. The exception is the kappa number plot. It is plotted against time and is measured at the bottom of the digester. This shows the steady state operation of the digester that yielded the concentration and temperature profiles. Since Kappa is a function of lignin concentration, its curve throughout the digester will have a similar shape as that of the lignin curves.

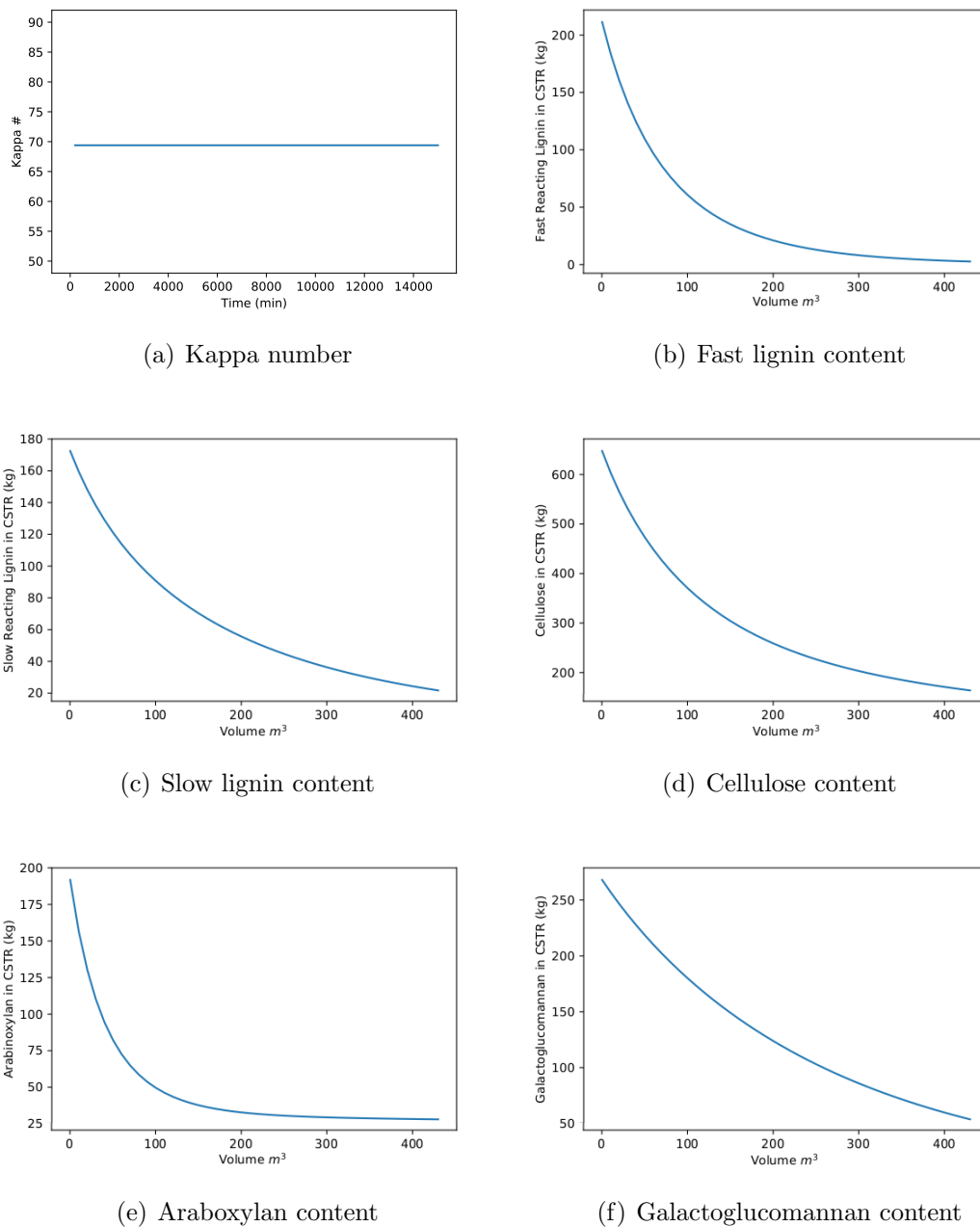


Figure 9: Wood component mass over volume of digester with steady state inputs.

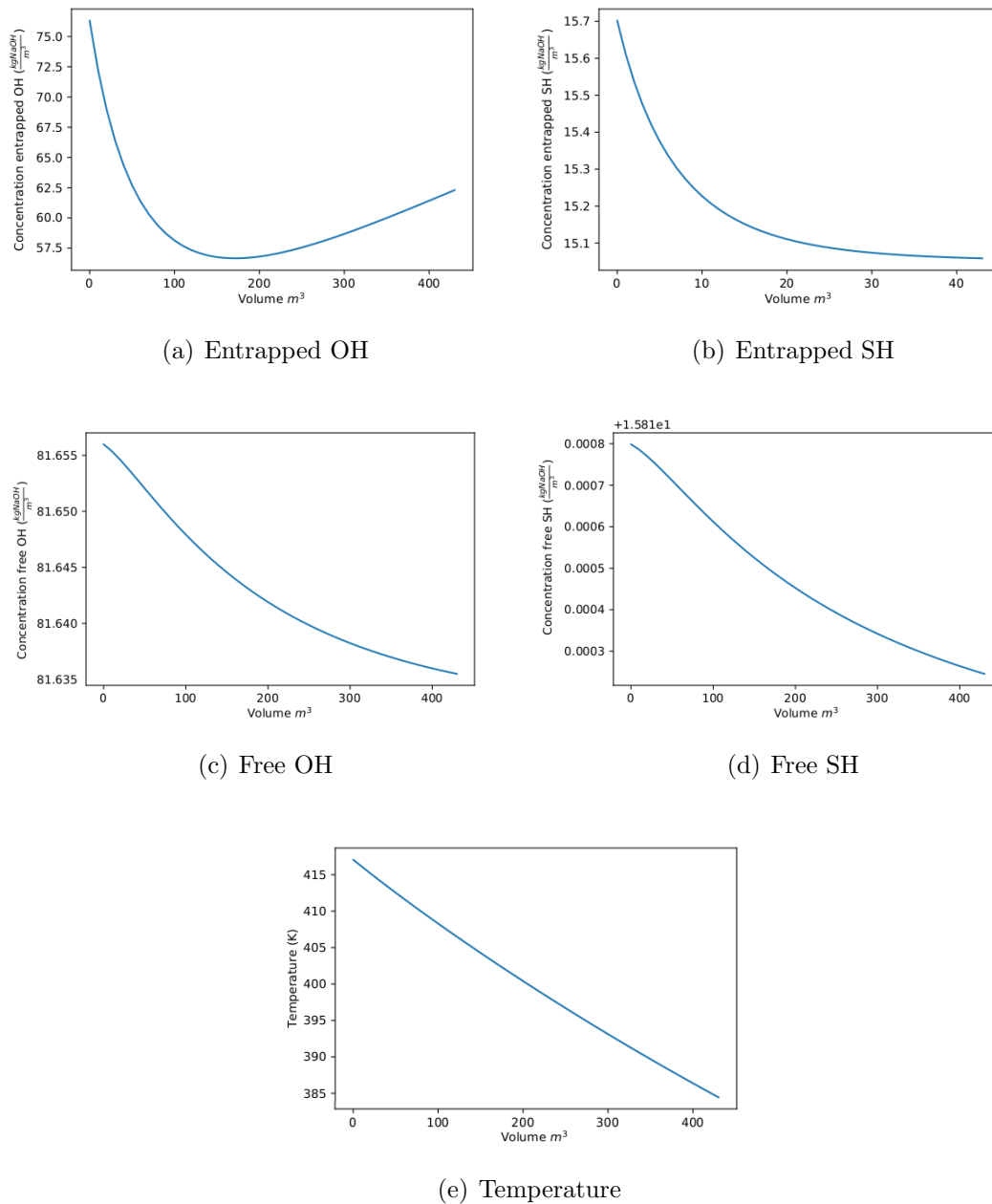


Figure 10: Caustic solution and temperature over digester volume with steady state inputs.

It is clear from the results that the model does indeed work as expected. It is clear from the wood component concentration curves that each wood component is decreasing throughout the column (as one would expect with the wood components reacting and breaking down). The Kappa value predicted also seems to be plausible or at least in the expected range (between 25 and 100). The dosing chemicals curves are less straightforward than the wood concentrations. The entrapped OH concentration has a minimum value in the middle of the column and the free SH decreases very slowly. This is surely due to some interesting model interactions brought about by the choice of the initial conditions. After this successful test, the model was applied to historic plant data.

5.2 Plant data comparison

The model as was used in Section 5.1 was applied to measured inputs taken directly from the Ngodwana digester. As mentioned in Section 4.2.3, the Kappa measured and predicted are not the same value and they are expected to differ to some incalculable degree. The implications of this will be discussed in Section 7.2.1. The predictions from the plant inputs were then plotted against the true measured plant outputs. This plant data has the same initial conditions as mentioned in Table 15, although the ‘Steady state inputs’ referred to, are now varying with only the first input being equal to the figures in the Table. The result is visible in Figure 11 below.

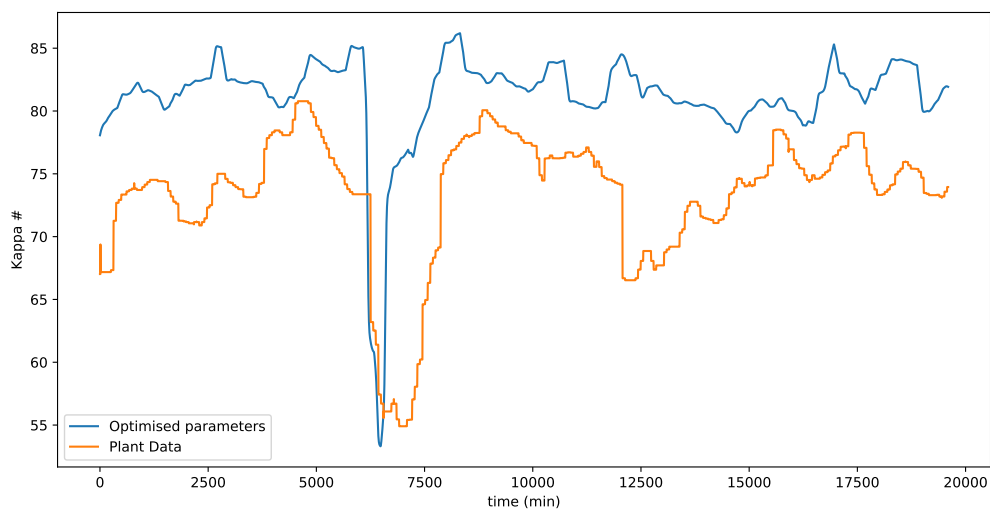


Figure 11: Kappa number predicted compared to real plant data.

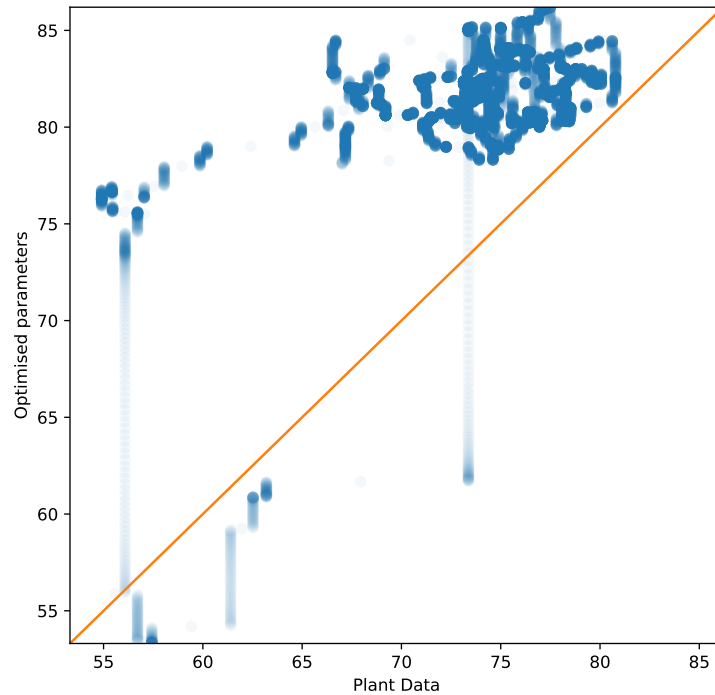


Figure 12: Parity plot of Kappa number predicted compared to real plant data.

It is clear from the results that, although the predicted Kappa and the actual Kappa have a similar form, they differ from one another. The average absolute error between the two fits are 7.88. There are various possible reasons for this. These include:

1. Some parameters are not completely known. The most notable of these are the heat transfer coefficients used in the energy balance as mentioned in Section 4.5. These 3 parameters greatly influence the temperature of the digester, which, in turn, greatly influences the rate of reaction and therefore the Kappa number in the digester. These parameters are therefore of great importance and need to be optimized to fit to real plant data.
2. None of the plant measurements are perfect. Noise, deviations and disturbances in both the input and output measurements are present and this will result in prediction that do not fit perfectly. The effect of this should, however, not be too noteworthy.
3. There will be some model inaccuracies (regardless of parameter values). These inaccuracies are mainly introduced by making simplifying assumptions about the digester operation in order to ease the complexity of the model. It is impossible to perfectly model every interaction in a digester and therefore, the prediction is expected to have some deviation from the measured plant data.

4. As will be further discussed in Section 7, the Kappa measurements, that the simulation is compared against, are not measured directly as the pulp exits the digester (as is modelled), but rather it is measured after the pulp has passed through the refiner section of the plant. The refiners alter the Kappa value of the pulp and the refiners have too little data to be adequately modelled. Because of this, the model accuracy will be measured against the plant Kappa measurements, although it is known that this is not equivalent to the Kappa number that is being modelled (leaving the digester).
5. Among the assumptions made, assumptions are made regarding the input concentrations of wood components as well as critical moisture content. This along with various other assumptions can skew the predictions away from the plant data.

In conclusion, the prediction is only as accurate as the information that can be provided. The model can, however be tuned (by altering the model parameters), to yield a prediction with an improved fit. The list below lists the model parameters, as well as discussing the whether they will be optimized for or not. The literature values of these parameters are given in Table 7, 8 and 10 in Section 4.5. optimization is often a fairly time-consuming approach and every variable (in this case, varying parameter) adds time to finding the optimized result. Because of this it was decided that not every parameter will be optimized for. Instead, the priority of varying the given parameter will be discussed and chosen from there.

Parameters not for optimization

The following parameters will not be optimized for since the values are known from previous studies:

Molar mass NaOH

Molar mass Na₂O

Universal gas constant

Pre-exponential constants

Activation energy

Consumption constants

The pre-exponential constants, the activation energies as well as the consumption constants have been studied by numerous authors (Rydholm, 1965; Christensen *et al*, 1982) and have always been reported to be values similar to these.

The following Parameters will not be optimized for since the values are known and not suspected of change:

Volume of the chip feeder This parameter is known from the chipper geometry. In reality there will be significant variation of the chip flow rate if the chip sizes vary at a constant chip feeder volume. For the sake of simplicity a constant chip size, was assumed

Liquor to wood ratio This value is controlled for by the plant. Proper control and little variance are assumed.

Liquid density The liquid density is not suspected to vary from the known value.

Wood density The wood density is not predicted to vary greatly from the reported value. In reality, wood density can vary depending on the size of the chips and whether flakes from the saw mill is added. For the sake of simplicity a constant chip size, was assumed.

Critical moisture content The critical moisture content of most wood species could not be found, however it was found that the moisture content of freshly sawed trees seldom exceed 66 %. The value of 65 % suggested by Smith & Williams (1974) will thus be used.

Parameters for optimization

The following parameters will be optimized for:

Mass fraction of component i in wood This could very possibly vary from the reported values since the wood types and ratios change with time. It will need to be optimized for.

Mass fraction non-reactive wood component This could very possibly vary from the reported values since the wood species and, therefore, composition in the plant is not constant. Some cellulose and galactoglucomannan will not react with the alkali and wood type has a influence on this. It will need to be optimized for.

Heat Capacities and Convective Heat Transfer Constant The heat capacity of the wood and liquid part of the pulp as well as the convective heat transfer constant mentioned in Section 4.5.4 are unknown and will need to be optimized for.

The result was 13 parameters that needed to be optimized for. Table 16 below contains the parameter values of the optimized fit, as well as literature values. Along with this, there are also a few other sets to illustrate the effects of various parameters on the fits. These parameters will be used in the model to give five different fits of the model to the data. This will then illustrate the effect of various parameter values on the model as well as show the difference in fit that can be achieved by using an optimised parameter set.

Table 16: Parameters used in fitting.

Run	x_i	x_∞	cp_w	cp_l	h
Literature	[0.15, 0.11, 0.43, 0.15, 0.17]	[0, 0, 0.25, 0.71, 0]	4	4	0.25
optimized	[0, 0.11, 0.51, 0.12, 0.27]	[0, 0.02, 0.01, 0.81, 0.05]	3.9	3.8	0.26
Set 1	[0, 0.11, 0.51, 0.12, 0.27]	[0, 0, 0, 0, 0]	4	4	0.25
Set 2	[0.15, 0.11, 0.43, 0.15, 0.17]	[0, 0, 0.25, 0.71, 0]	2	2	0.3
Set 3	[0.15, 0.11, 0.43, 0.15, 0.17]	[0, 0.02, 0.01, 0.81, 0.05]	4	4	0.25

Below is the results of the various fits, along with their average absolute error, to illustrate the accuracy of the fit. For the literature values and the optimized values there will also be a parity plot for additional analysis

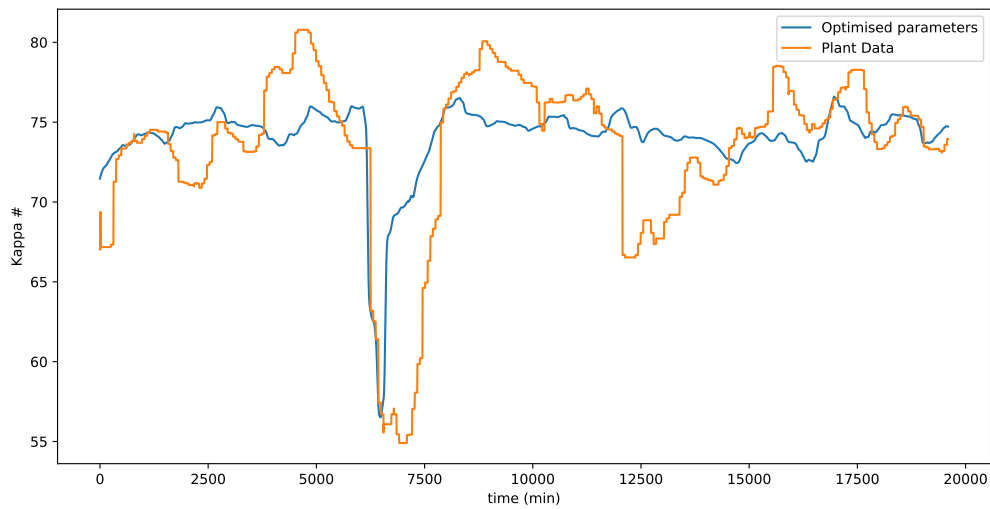


Figure 13: Kappa number predicted by optimized parameters compared to real plant data.

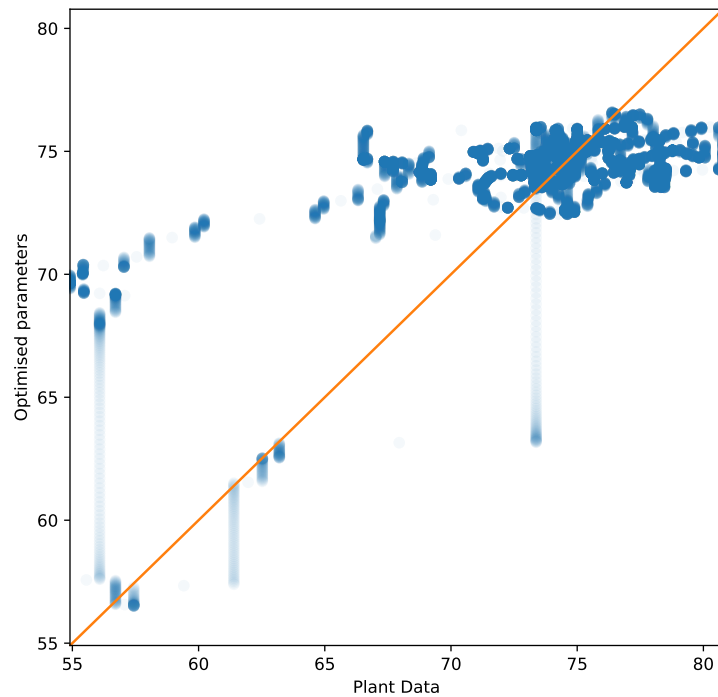


Figure 14: Parity plot showing Kappa number predicted by optimized parameters compared to real plant data.

From comparing the Kappa plots in Figures 11 and 13 it is clear that optimized parameters does not exhibit the bias that is seen in the literature values. This also shows clear when comparing the parity plots in Figures 12 and 14. In Figure 12 that shows the parity plot of the literature values, it is clear that the majority of the data points are above the $x = y$ line, whereas in Figure 14, the data points are shared almost equally between the top and bottom of the $x = y$ line, showing a clear reduction in bias. This is also reflected in the average absolute error that is reduced from 7.88 for the literature values, to 2.87 for the optimized values for this data set.

It is known that R^2 is a valuable tool for determining the goodness of a linear fit, however it is not valid for non-linear fits, such as this one (Spiess & Neumeyer, 2010). Because of this, the absolute average error will be used as measure of goodness of fit instead.

The results of other sets with their parameters tabled in Table 16, is visible below:

Set1

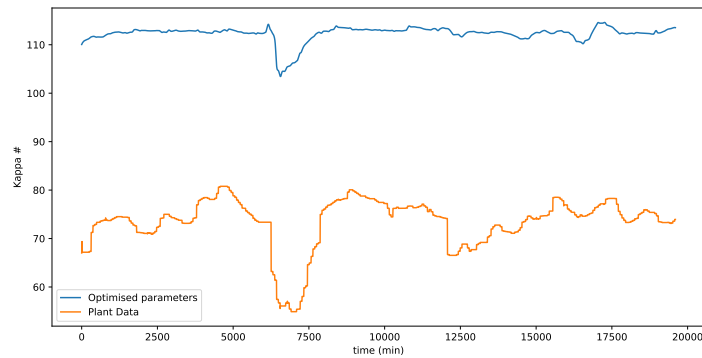


Figure 15: Kappa number predicted by Set 1 parameters compared to real plant data.

Set 1 was simulated with the assumption that all the wood components would react completely. This was done by reducing all the values of x_{∞} to zero. The result is a Kappa number prediction that is a lot higher than the plant data. It is because, with the limit f reaction removed, both cellulose and araboxylan can now react more completely. They both react quicker than slow lignin, therefore, using the caustic solution and resulting in more unreacted lignin and a higher Kappa number.

Set2

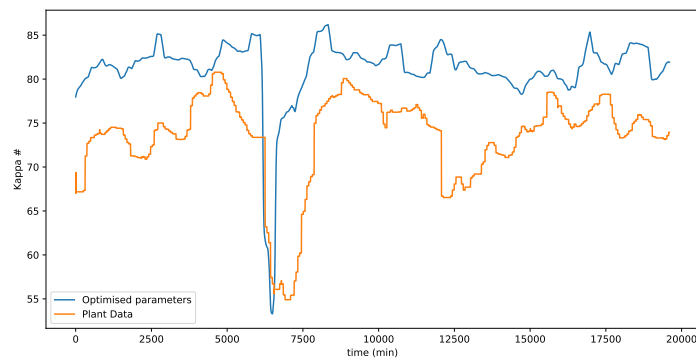


Figure 16: Kappa number predicted by Set 2 parameters compared to real plant data.

Set 2 was simulated with a lower heat capacity and higher h value. The result is that the pulp slurry cools down faster throughout the column, both because of the lower heat capacities well as the higher convective heat transfer constant. The resulting cooling slows down the rate of reaction of all components in the digester, resulting in less lignin reacting and raising the Kappa value. This is why the Kappa value is higher than the plant data.

Set3

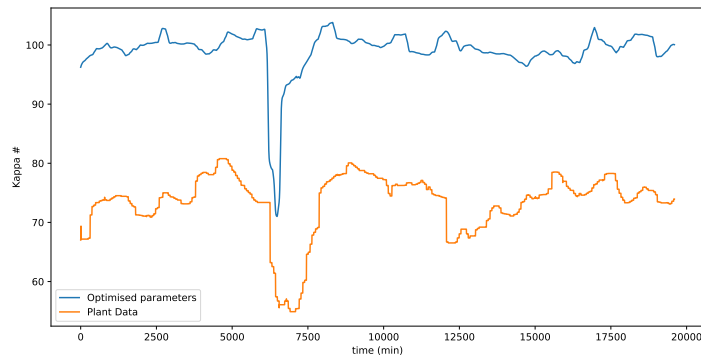


Figure 17: Kappa number predicted by Set 3 parameters compared to real plant data.

Set 3 used the x_{∞} of the optimized parameters with the wood composition of literature. The result is a higher Kappa than what was seen with the literature plot. This is because, similarly to set 1, the x_{∞} value of cellulose came down and although araboxytan's went up, it makes up a much smaller part of the wood than cellulose. Because of this, the cellulose reaction could run faster and longer than with the literature values and use more caustic solution, leaving less for the reaction of lignin, raising the Kappa number.

It is clear that none of these 3 sets are better than literature values, however it does show the large differences even small changes in parameter values can make.

6 Model enhancements

From Section 5.2 above, it is clear that the model predicts the true process quite accurately. In any model however, there are some improvements that can be made, above and beyond tuning the parameters to obtain a good fit. The methods that will be implemented here are state estimation (as discussed in Section 2.9) and adaptive control (as discussed in Section 2.10). The design and implementation of these methods will be discussed below.

6.1 State estimation

In systems such as this, where not all the states are closely measured, the need sometimes arises to estimate the states of the system, to ensure that the states used by the model are still accurate. State estimators are discussed in more detail in Section 2.9 above.

6.1.1 Need for state estimation

In this model there are numerous internal states throughout the column that are not measured. These states are: mass of wood component i in CSTR, caustic concentrations in entrapped and free liquor in the CSTR as well as CSTR temperature. This yields 10 (5 wood components, 2 entrapped concentrations, 2 free concentrations and temperature) per CSTR and currently the 430 m³ of the digester are divided into 10 m³ sections, yielding 43 CSTRs and therefore 430 states. Of these states, only the lignin mass fraction (sum of wood component 1 and 2 per kg pulp) can be deduced from the Kappa number measurement. The large number of unmeasured states pose a problem. If some or other internal state variable in the model, due to some modelling inaccuracy or assumption, changes in a way that is different to the true changes in the digester, that state might become a source for inaccuracy in itself. This tends to become worse and worse over time of the simulation, as the state variable deviates further and further from the true value, eventually becoming absurd and driving the model to uselessly low accuracy. A solution to this problem is to periodically (perhaps daily or weekly depending on the intensity of the problem) use the measurements obtained from the various outputs and use this to estimate the states of the system. The inferred model states then replace the model states used by the model up and to that point. This then updates the states of the model to reasonable values and ensures that the system predictions does not drift away from the true value too drastically.

The two main options for state estimation of a non-linear system are, using modified Kalman filters (EKF or UKF) or using moving horizon estimation (as mentioned in Section 2.9). From the literature in Section 2.9 it is clear that the MHE approach is superior to the modified Kalman filters in terms of performance. Because of this, it was

decided that it would be used as the state estimator in this model.

6.1.2 Method

The internal states of the model can be seen in Table 15 and is summarized in Table 17 below. These states refer to the internal variables of every one of the discretized volume sections (or CSTRs).

Table 17: States of every CSTR segment in digester.

Symbol	Description	Unit
OH_e	Concentration entrapped OH in CSTR	$\frac{kg_{NaOH}}{m^3}$
SH_e	Concentration entrapped SH in CSTR	$\frac{kg_{NaOH}}{m^3}$
OH_f	Concentration free OH in CSTR	$\frac{kg_{NaOH}}{m^3}$
SH_f	Concentration free SH in CSTR	$\frac{kg_{NaOH}}{m^3}$
T_c	Temperature of CSTR	K
m_{w1}	Weight of slow lignin in CSTR	kg
m_{w2}	Weight of fast lignin in CSTR	kg
m_{w3}	Weight of cellulose in CSTR	kg
m_{w4}	Weight of araboxytan in CSTR	kg
m_{w5}	Weight of galactoglucomannan in CSTR	kg

As mentioned above, there are ten states for every CSTR segment in the digester and typically 43 CSTRs, yielding 430 internal states. 430 variables would require an enormous amount of computational time to solve. To cut down on the number of required variables, it was decided to approximate the internal states of the various CSTRs. After looking at Figure 9, it became clear that most of the states of the digester follow a smooth curve through the CSTRs. This presented an opportunity to reduce the number of parameters that needed to be optimized for. It was decided to rather fit the parameters of the various curves and approximate the CSTR values using it than to fit each and every CSTR parameter value. For simplicity, it was decided to approximate these curves as exponential functions, allocating 3 variables to each curve such that each curve resemble:

$$ab^{-x} + c \quad (71)$$

with a, b and c being these variables. Alternative forms, such as polynomials were also considered, however the exponential form showed the best correlation. This resulted in 10 states (outlined in Table 17), each with 3 variables (a, b and c) to fit their continuous curve profile. This results in 30 variables to be optimized for in total vs. the initial 430. This made a vast improvement in terms of simulation time. It is also believed that the values obtained using this method would be representative of reality and therefore it

should not greatly impact the accuracy of the prediction. The initial 430 variables can in turn then be calculated using the curves as given by the 30 optimized parameters. It should be noted again that the model reaction kinetics were developed by empirically fitting equations to measurements that were made. The reaction kinetics predict the main wood components well but the model does not predict the rate of reaction of all the byproducts that form. the model does not have equations for the byproducts and will therefore not be able to track their concentrations.

6.1.3 Results

After implementation of the MHE it was applied such that the initial conditions of the simulation was optimized for before starting the simulation, instead of using sensible guessed values as initial conditions. The result is visible in Figure 18 below:

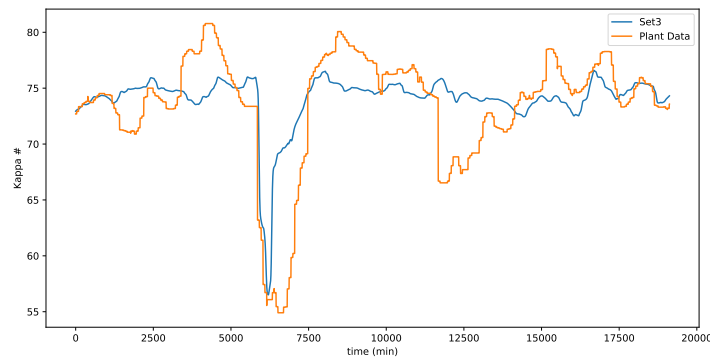


Figure 18: Kappa number predicted by optimized parameters with MHE initial values compared to real plant data.

The resulting average absolute error is 2.75, which is better than without the MHE, although it would seem from both the plot and the error, that it did not make a very large difference. However, although the difference is not large, it is important to ensure the internal states are accurately estimated at regular intervals.

6.2 Adaptive control

As discussed in Section 2.10, not all parameters truly stay constant at all times. While there are some parameters, such as the rate of reaction, pre-exponential constants as well as the activation energies, many other do change (very little normally) over time. There are various possible reasons for this, such as for example:

- Wood composition could gradually change as the season change.
- Ambient temperatures with the seasons.

- Different wood types might be used or mixed with assumed wood type.
- The critical moisture content of wood might change as wood type change.
- The unreacted fraction of wood components might change.

All of these and similar situations could change the assumed parameters over time. Because of this, it is valuable to periodically (typically once every month or three), take a historic data set and optimize the parameters to fit the data. This will ensure that the parameter drifts are accounted for and that changing parameters do not cause inaccuracies in the system. Another idea that builds on this is to rather optimize for one variable at a time over a much shorter time. This is less accurate, however it has the advantage that there is no need to run one large optimization instance that could take a relatively long time to complete. Rather it runs faster, smaller optimizations more frequently. This should also keep the predictions closer to optimal for the greater part of digester operation resulting in greater long-term model accuracy. This also allows for the possibility to optimize certain parameters, such as those that are known to drift more rapidly, more frequently than others, such as parameters that are known to drift less frequently, less drastically or whose drift has a smaller effect on the overall model accuracy.

It was implemented on the model, however the data sets that were available were not for long enough periods that a significant change in parameters could be noticed over the time available. Figure 19 below shows an extreme example of how this would look. Figure 19 is created by simulating the model with erroneous parameters and then optimizing parameters at 4800 minutes to illustrate the difference that it would make. Parameter optimization yielding different parameters should find benefit in also running a MHE close to this time, otherwise the ill effect of the old parameters will be propagated further, even though the parameters are now corrected.

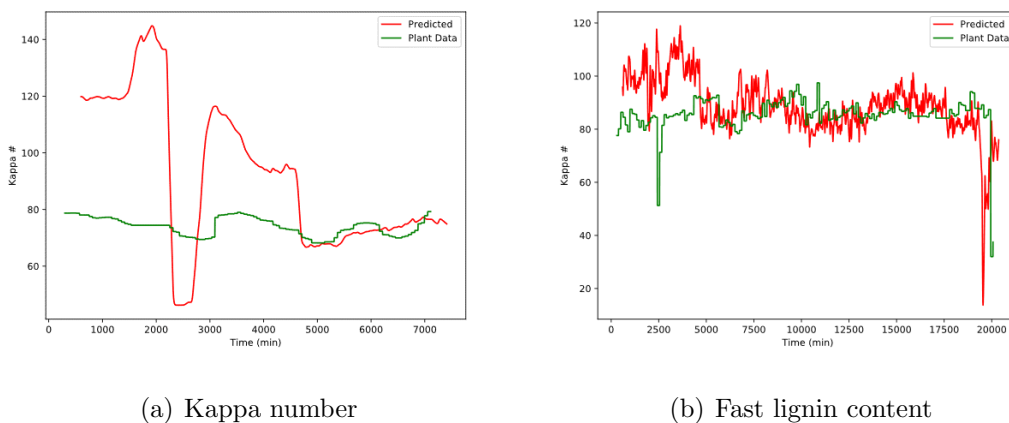


Figure 19: Exaggerated examples of the possibilities introduced by adaptive control.

7 Data handling

To achieve the aforementioned results, numerous datasets needed to be chosen, refined and cleaned to ensure a precise measure of the model accuracy. This is mainly due to inconsistencies in plant measurements, such as measurement noise, measurement downtime as well as general measurement inaccuracies.

7.1 Data processing

All the relevant input and output data from the plant were obtained from the digester historian at Ngodwana. This yielded a year and 6 months worth of data. As is common with data obtained from an industrial process, the data was not ready for use in the form it was received. The data needed to be cleaned and scrubbed before it could be used to test the model. This cleaning process consisted of 2 parts.

1. At various times it would happen that certain measurements yielded no or nonsensical measurements. At other times it would also happen that the same measurement output is reported for several days on end and this measurement was often nonsensical. This is common on industrial plants but it creates difficulty when testing. To solve this the large data set was divided into data sections that did not contain these values. This yielded a subset of smaller data sets without this problem.
2. At some times, some measurements would measure values that were clearly higher or lower than can be reasonably expected. It only measured these values for short intervals before continuing as expected. It is also known that measurement devices are prone to measurement noise that need to be rectified. Because of the slow dynamics of the system, it was decided that both of these problems can be mitigated by subjecting the data to a rolling median filter. This filter moves (or rolls) over the data and adjust any value to be equal to the median of the previous N data points (where N is the filter range). The rolling median filter was chosen above the rolling mean filter because the rolling mean is less susceptible to outliers and quick changes in variables are not expected. This smoothed out the noise as well as the outliers of the system.

7.2 Kappa number measurements

As mentioned briefly in Section 4.2.3, the Kappa number of the pulp (the main model output) is measured at three different locations on the plant. These locations are visible in Figure 20. The model is designed to predict the Kappa number of the pulp as it exits the digester. None of these however, measure the Kappa number directly as the pulp exits the digester. Instead, two of the measurements are taken directly after the refiners,

with the third being taken after several additional processes. Because of the distance of the third analyser from the digester, it is suspected that it will be of little use, however it will still be investigated. The measurement locations of the first two can be seen on Figure 20 below. The third measurement is too deep into the plant to reasonably show alongside the first two in a figure.

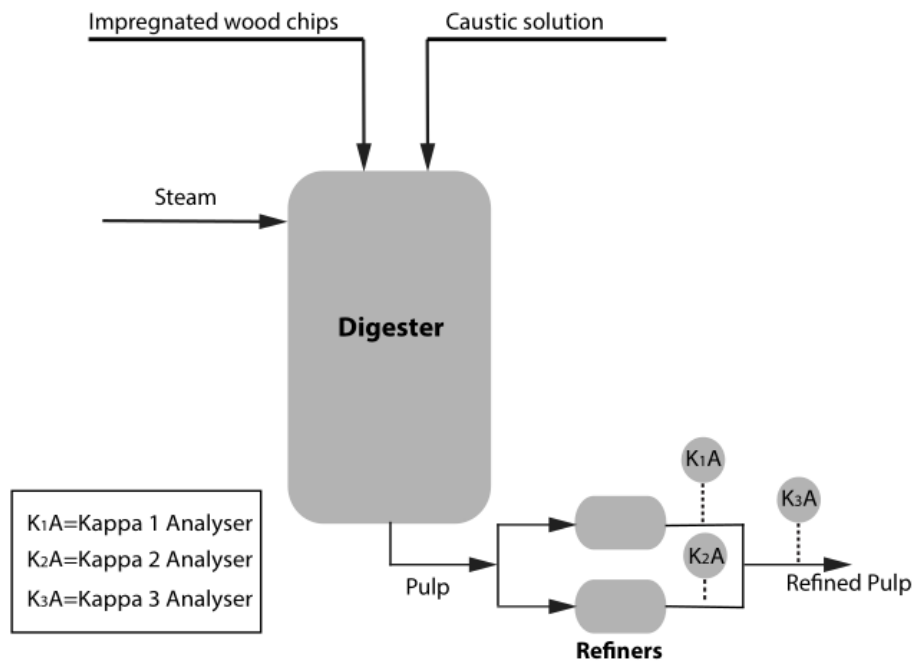


Figure 20: Kappa analyser 1, 2 and 3 location in relation to the digester.

7.2.1 Kappa measurement inconsistency

This caused a challenge since the first two do not yield the same results (since the refiners are not operated identically and the refining process alters the Kappa number). The third analyser was only installed fairly recently and therefore does not have a large amount of data for comparison. What could be compared, however, seemed to indicate that its reading also differs from the other two. The comparison of the data can be seen in Table 18 below. These comparisons were done for all three over the same time period. Three data sets were chosen to represent the data.

Table 18: Measures of Kappa measurement similarity.

Number	Measure	Data sets being compared		
		K_1 and K_2	K_1 and K_3	K_2 and K_3
1	Average relative error	0.087	0.208	0.130
	Average absolute error	5.1	11.2	6.1
2	Average relative error	0.071	0.157	0.081
	Average absolute error	5.3	11.7	6.4
3	Average relative error	0.058	0.263	0.195
	Average absolute error	3.7	16.6	13.0

The plot of the first case along with the three parity plots are given in Figures 21 and 22 below. This serves as a visual representation of some of the data in Table 18 above.

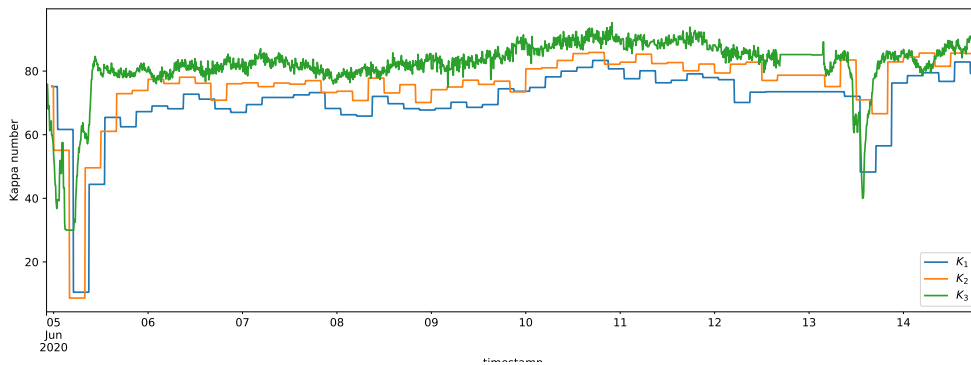


Figure 21: Kappa measurements over time for a randomly chosen data set.

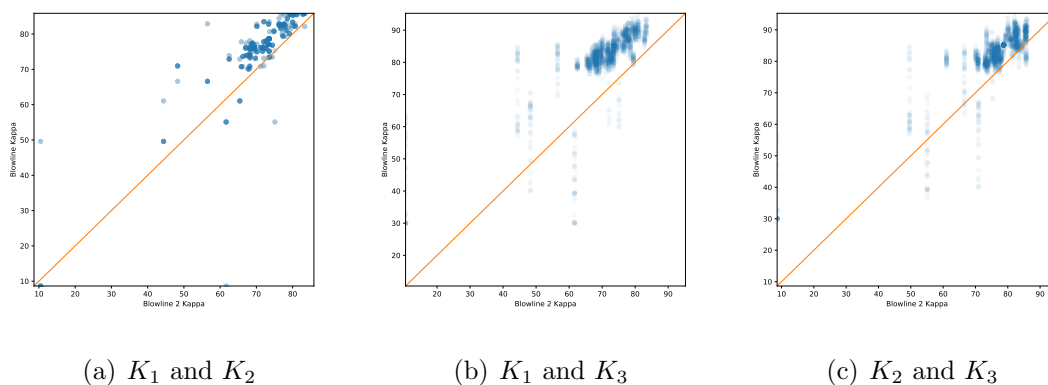


Figure 22: Parity plot showing similarity between Kappa measurements over time for a randomly chosen data set.

From this it is clear that none of the Kappa numbers resemble each other enough to assume them equal to one another. The model accuracy is measured against the plant Kappa number, adding weight to this challenge.

7.2.2 Solution

Numerous attempts were made to correct for these measurement inaccuracies, however, since not enough data was available to model the refiners with any amount of detail, none were deemed to improve the accuracy of the measurement obtained from the Kappa analysers. However, since the model will primarily be used predicatively, it was decided that the ability to detect changes in Kappa is more important than accurately predicting Kappa. Because of this and the inconsistent data, it was decided to compare the plant data to a single measurement. For this measurement, the Kappa measurement of analyser 1 was chosen. This was because it had larger sections of usable measurements than its counterpart on the other refiner. It also had more available data than the third analyser, therefore making the choice more appealing. All the results from Sections 5 and 6 are given with the plant Kappa number equal to this first Kappa measurement.

8 Conclusion

A mathematical model of a continuous Kraft wood digester was constructed and tested. This model relies heavily on the work done previously by Christensen *et al* (1982). The batch Kraft digester model developed by Christensen *et al* (1982) was used and adapted to model a continuous Kraft wood digester at Ngodwana, South Africa. The adaptation centres around utilizing the method of lines to account for changes in both time and height of the digester simultaneously. The results from the model were able to simulate the Kappa number of the digester accurately to an average absolute error of 7.88 that was reduced to 2.87 after certain process parameters have been optimized for. A moving horizon state estimator was introduced into the model in an effort to keep internal state prediction accurate. This addition brought the average absolute error down further to 2.75. Adaptive control was also additionally implemented into the model. The plant data, that the model was compared against to determine its accuracy, was filtered with the use of a rolling median filter to reduce the influence introduced by noisy and infrequent measurements. The model provides Sappi with numerous insights. First and foremost, the model is used to predict the future Kappa number. This enables the plant operator to take earlier action to correct the control conditions of the digester when it is predicted that the Kappa number will deviate from the specified controlled value, reducing Kappa variability. The model also supplies Sappi with a mathematical representation of the digester that can be used to increase understanding of its operation. This is an advantage of using a first principles model as opposed to, for instance, a neural algorithm or other machine learning modelling alternatives.

References

- Bavdekar, VA, Gopaluni, RB and Shah, SL (2013) “A Comparison of Moving Horizon and Bayesian State Estimators with an Application to a pH Process” *IFAC Proceedings Volumes*, 46, (32).
- Bhartiya, S, Dufour, P and Doyle, FJ (2003) “Fundamental thermal-hydraulic pulp digester model with grade transition” *AIChE journal*, 49, (2).
- Christensen, T, Albright, LF and Williams, TJ (1982) *A mathematical model of the kraft pulping process*, Purdue Laboratory for Applied Industrial Control.
- de Vaal, P and Sandrock, C (2007) “Control of a batch pulp digester using a simplified mechanistic model to predict degree of polymerisation” *Computers and Chemical Engineering*, 31, (10).
- Ek, M, Gellerstedt, G and Henriksson, G (2009a) *Pulp and paper chemistry and technology. Volume 1, Wood chemistry and wood biotechnology*, De Gruyter.
- Ek, M, Gellerstedt, G and Henriksson, G (2009b) *Pulp and paper chemistry and technology. Volume 2, Pulping chemistry and technology*, De Gruyter.
- Eliot, S and Rose, J (2009) *A Companion to the History of the Book*, Wiley-Blackwell ISBN: 978-1-4051-9278-1 URL: <https://app.knovel.com/hotlink/toc/id:kpTAC00009/techniques-adaptive-control/techniques-adaptive-control>.
- Gibson, L (2012) “The hierarchical structure and mechanics of plant materials” *Journal of the Royal Society*, 9, (76) DOI: <https://doi.org/10.1098/rsif.2012.0341>.
- Gullichsen, J and Fogelholm, C (1999) *Chemical pulping, volume 2 of Papermaking science and technology*, Fapet Oy.
- Gustafson, RR, Sleicher, CA, McKean, WT and Finlayson, BA (1983) “Theoretical Model of the Kraft Pulping Process” *Industrial & Engineering Chemistry Process Design and Development*, 22, (1).
- Hagberg, B and Schöön, N (1973) *Kinetical aspects of the acid sulfite cooking process: Part 1: Rates of dissolution of lignin and hemicellulose*, Svensk Papperstidning.

Härkönen, EJ (1987) “A mathematical model for two-phase flow in a continuous digester” *Tappi journal*, 70, (12).

Haseltine, EL and Rawlings, JB (2005) “Critical Evaluation of Extended Kalman Filtering and Moving-Horizon Estimation” *Ind. Eng. Chem. Res.* 44, (8).

Kayihan, F, Gelormino, MS, Hanczye, EM, Doyle, FJ and Arkun, Y (1996) “A Kamyr Continuous Digester Model for Identification and Controller Design” *IFAC Proceedings Volumes*, 29, (1).

Kilian, A (1999) “Control of an acid sulphite batch pulp digester based on a fundamental process model” Master’s Thesis, South Africa: University of Pretoria.

Levenspiel, O (1999) *Chemical Reaction Engineering*, Wiley.

Michelsen, FA (1995) “A dynamic mechanistic model and model-based analysis of a continuous Kamyr digester” PhD Thesis, Norway: University of Trondheim.

Patt, R and Kardsachia, O (1991) ”Pulp” in *Ullmann’s Encyclopedia of Industrial Chemistry*, VCH Publishers.

Pikka, O and Andrade, MA de (May 2015) “New developments in pulping technology” in: *Proceedings of the 7th ICEP— International Colloquium on Eucalyptus Pulp*.

Rahman, M, Avelin, A and Kyprianidis, K (2019) “An Approach for Feedforward Model Predictive Control of Continuous Pulp Digesters” *Processes*, 7, (9).

Rakovic, SV and Levine, WS (2018) *Handbook of Model Predictive Control*, Springer International Publishing AG.

Rippen, DV (1982) “Simulation of Single- and Multiproduct Batch Chemical Plants for Optimal Design and Operation” *Computers and Chemical Engineering*, 7, (3).

Rydholm, SA (1965) *Pulping Processes*, Wiley.

Sandrock, C (2003) “Implementation and performance analysis of a model-based controller on a batch pulp digester” Master’s Thesis, South Africa: University of Pretoria.

Sappi (2020) *A leading global provider of sustainable woodfibre products and solutions.*
URL: sappi.com (visited on 02/18/2020).

Schiesser, WE and Griffiths, GW (2009) *A Compendium of Partial Differential Equation Models: Method of Lines Analysis with Matlab*, Cambridge University Press.

Seborg, D, Edgar, T, Mellichamp, D and Doyle, F (2011) *Process dynamics and control*, John Wiley & Sons.

Smith, C and Williams, T (1974) *Mathematical modelling, simulation and control of the operation of a Kamy continuous digester for the kraft process*, Purdue Laboratory for Applied Industrial Control.

Spieß, AN and Neumeyer, N (2010) “An evaluation of R2 as an inadequate measure for nonlinear models in pharmacological and biochemical research: a Monte Carlo approach” *BMC Pharmacol*, 10, (6).

Stephens, M (2017) “Implementation of a pulp digester model with adaptive parameter estimation” Master’s Thesis, South Africa: University of Pretoria.

VanDoren, VJ (2003) *Techniques for Adaptive Control*, Elsevier ISBN: 978-0-7506-7495-9 URL: <https://app.knovel.com/hotlink/toc/id:kpTAC00009/techniques-adaptive-control/techniques-adaptive-control>.

Varshney, D, Patwardhan, SC, Bhushan, M and Biegler, LT (2019) “Batch and Moving Horizon Estimation for Systems subjected to Non-additive Stochastic Disturbances” *IFAC PapersOnLine*, 42, (1).

Watson, E (1992) “Mathematical modelling and experimental study of the kinetics of the acid sulphite pulping of Eucalyptus wood” Master’s Thesis, South Africa: University of Natal.

Wisniewski, PA, Doyle, FJ and Kayihan, F (1997) “Fundamental continuous-pulp-digester model for simulation and control” *AIChE Journal*, 43, (12).